AstroSat / CZT Imager

Dipankar Bhattacharya
IUCAA, Pune India

The primary objective of AstroSat is simultaneous, broadband (UV-hard X) Timing and Spectroscopy

The UV Imaging Telescope is also a good instrument for studying the distribution of hot gas/ star formation.

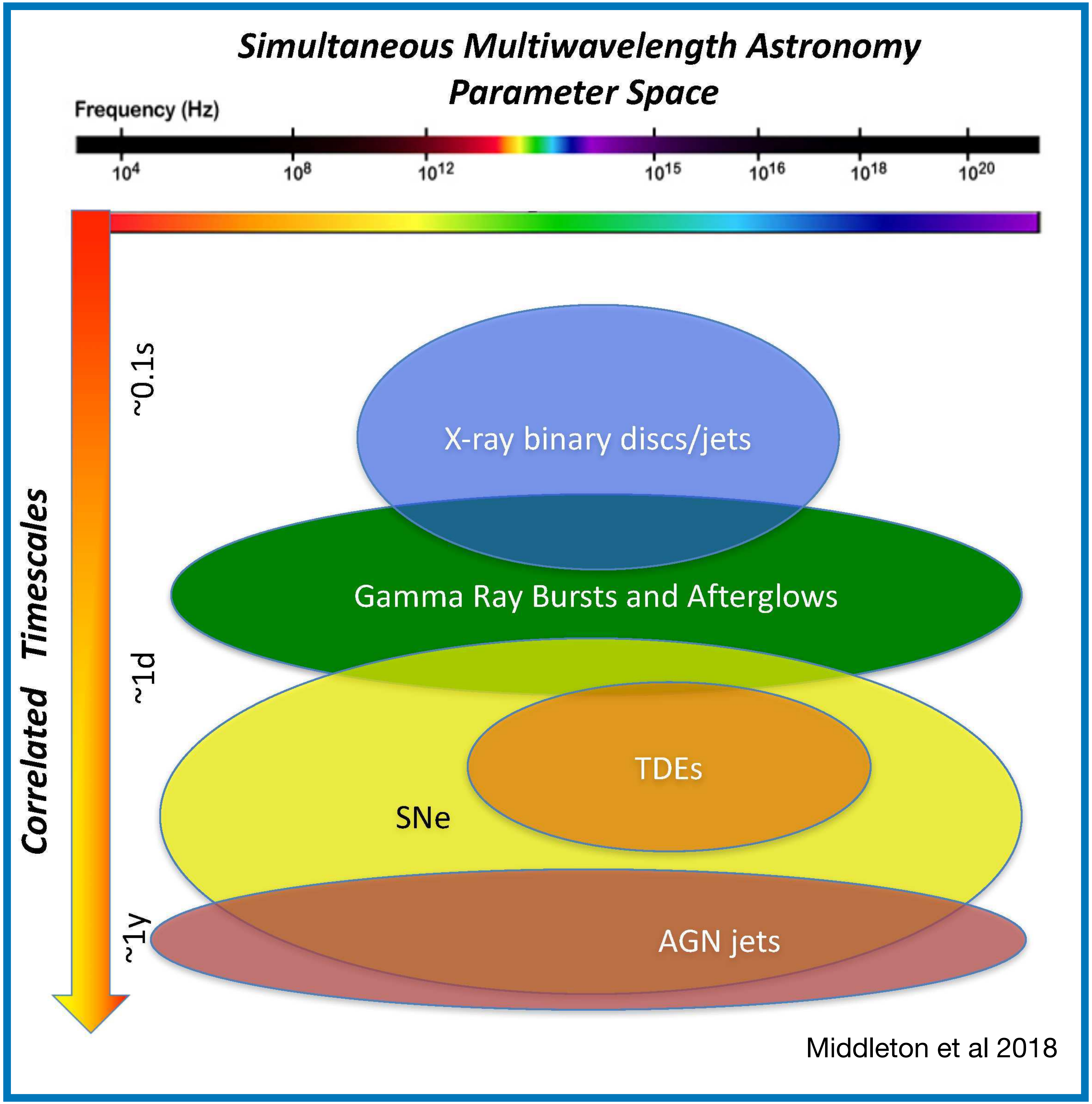

ASTROSAT

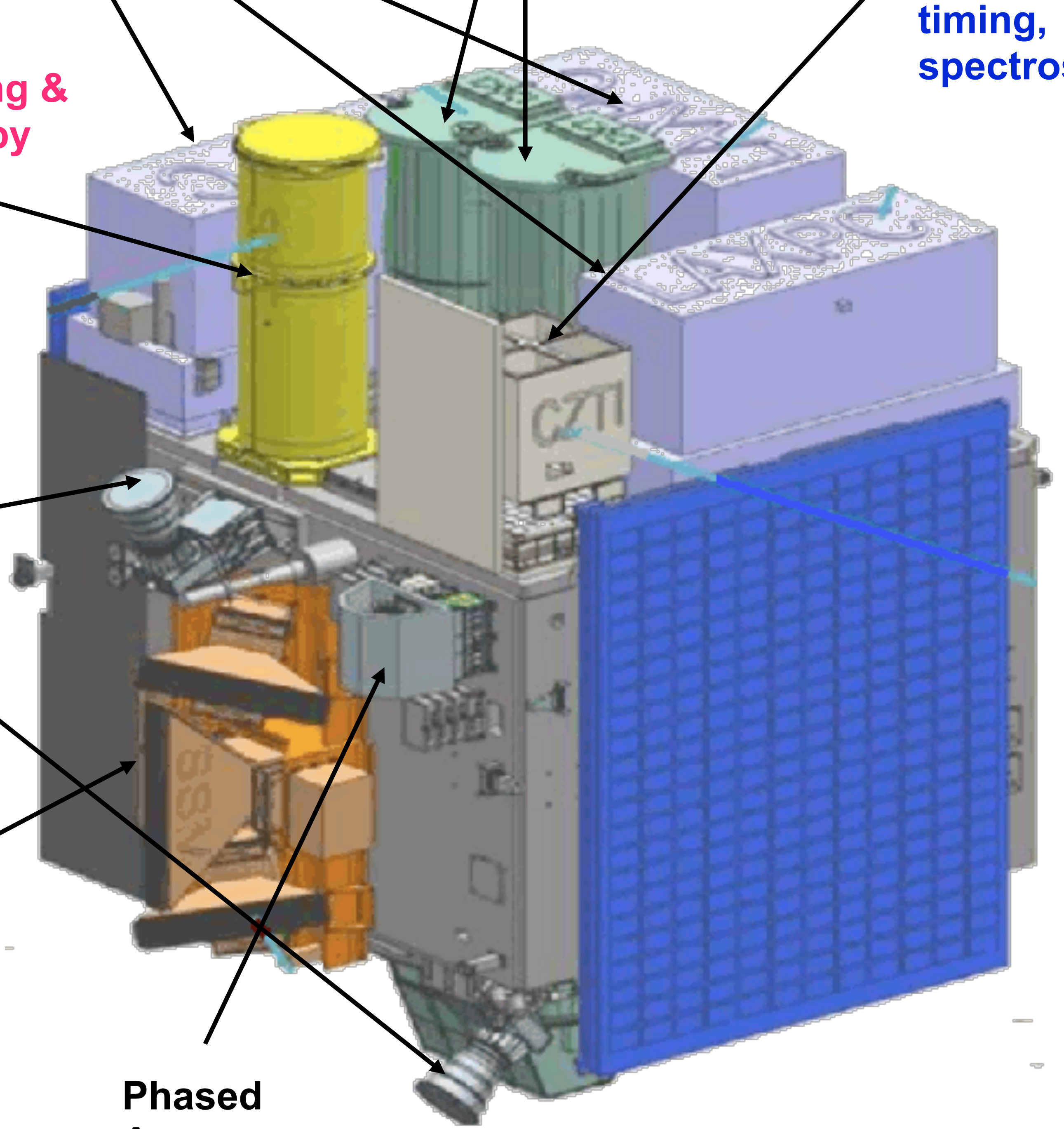

ISRO / http://astrosat.iucaa.in/

Launched 28 Sep 2015

Orbital period 98 minutes

Open proposal based science operation since Oct 2016

Annual cycle based proposals;

ToO proposals may be submitted at any time

All instruments provide individual photon recording

ASTROSAT orbit

650 km altitude: stable and limited background

6 deg inclination: avoids most of South Atlantic Anomaly

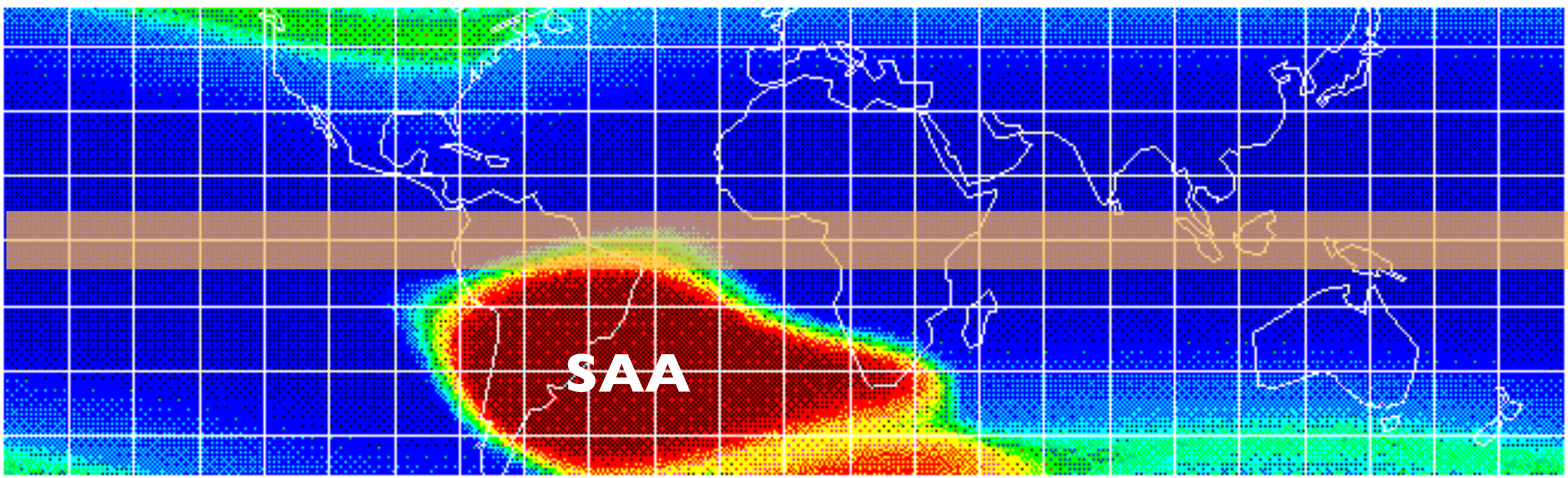

Wikipedia

Astrosat co-pointed FOVs

Satellite pointing accuracy: ~ 3 arcmin

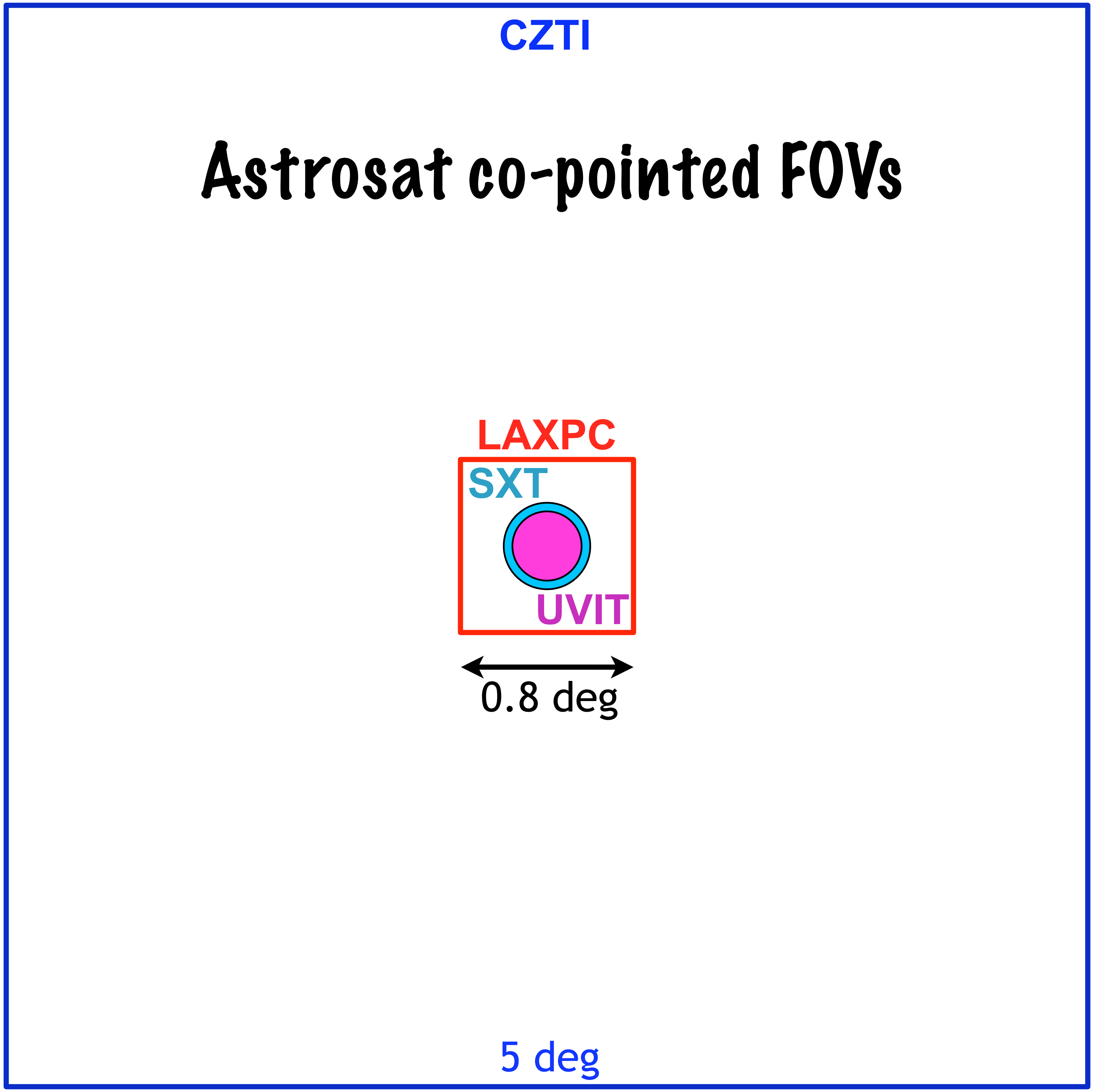

View constraints:
Sun > 65^{o}
Moon > 20^{o}
Earth limb > 12^{o}
Ram angle > 12^{o}

CZTI:
128x128 array + Coded Mask

LAXPC:
Collimator

UVIT:
MCP+CMOS 512x512

SXT:
Foil Mirrors + 600x600 CCD

Astrosat: angular resolution of co-pointed instruments

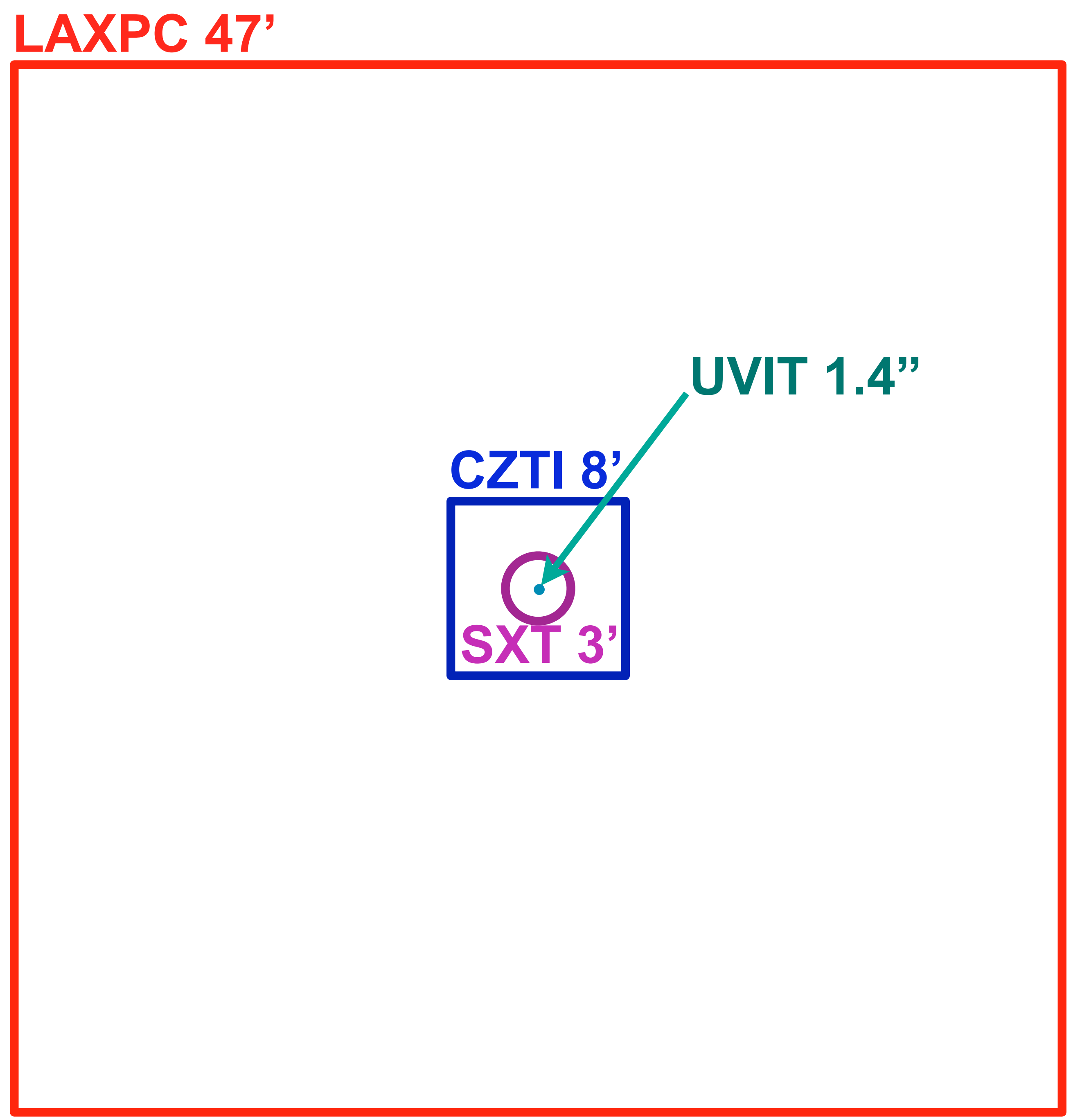

Spectral Coverage and Time Resolution available in some active space borne observatories

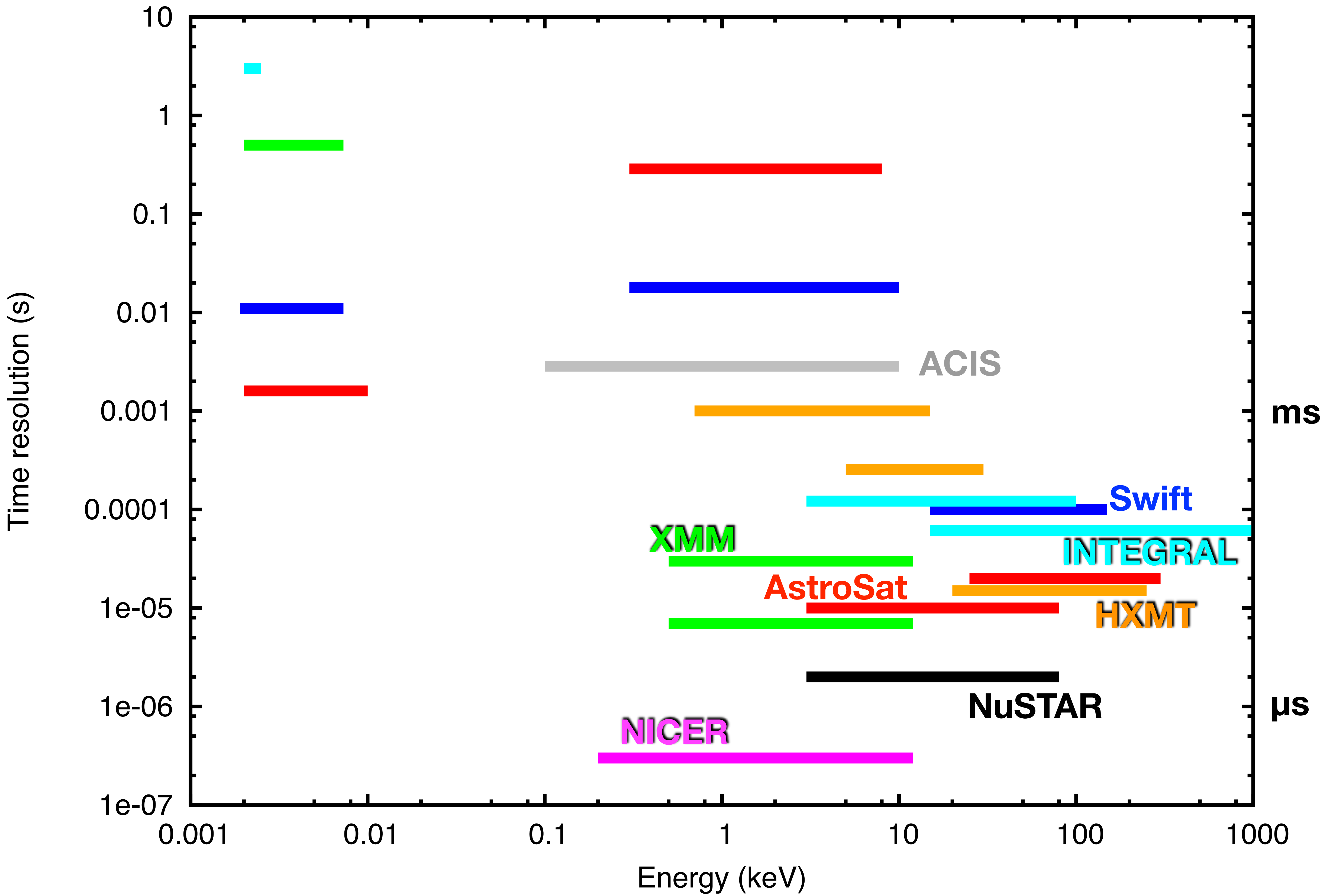

Fast timing also requires high photon collection rate, demanding a large effective area

Effective area of AstroSat compared with other missions

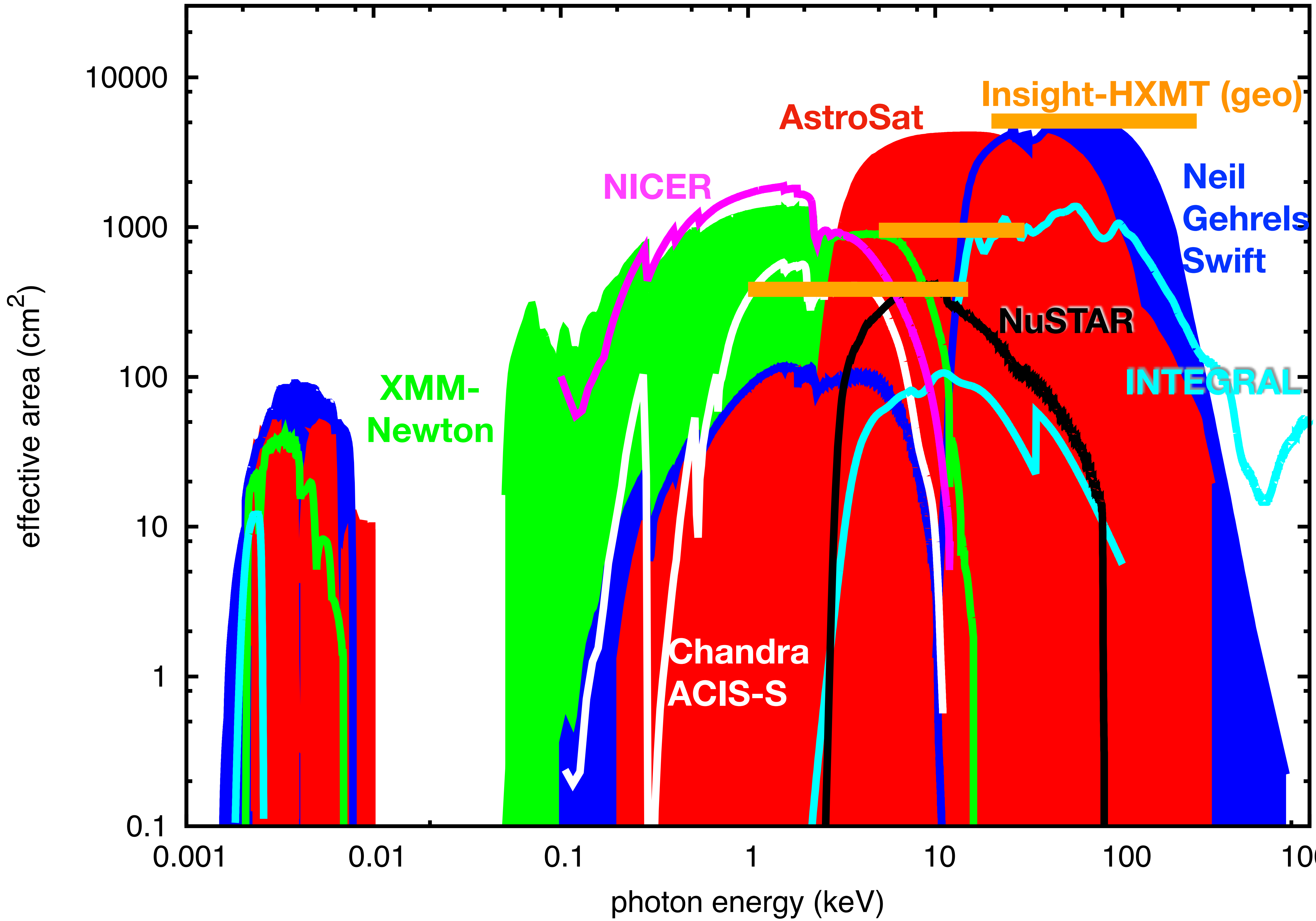

UltraViolet Imaging Telescope (UVIT)

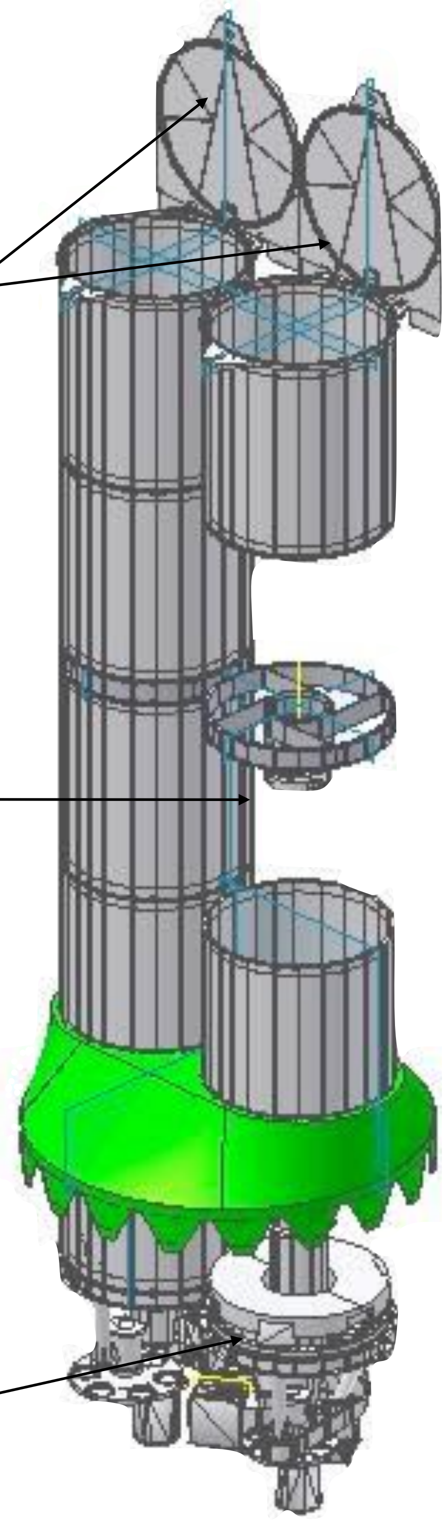

Detectors: Microchannel Plate + Photon counting CMOS sensor (STAR250)

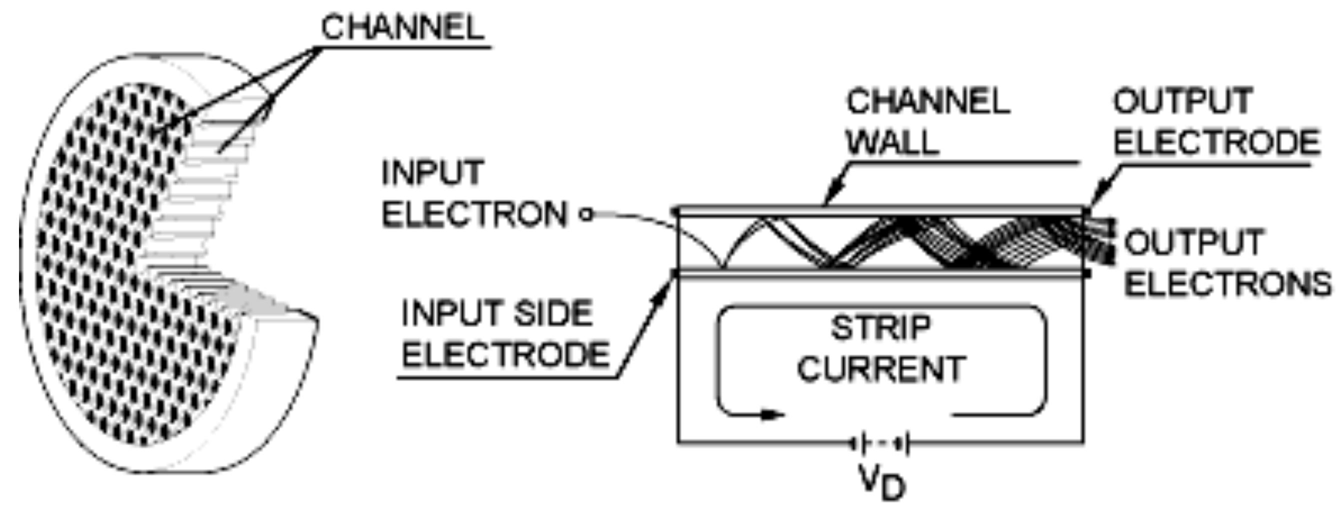

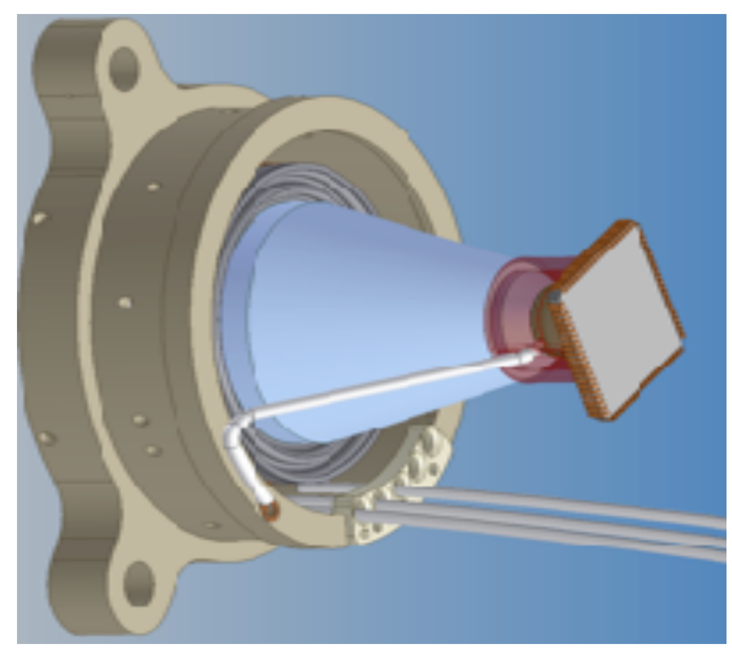

UVIT team / S N Tandon

3 channels: FUV,NUV,VIS simultaneous, multiple filters in all, gratings in FUV, NUV

Currently NUV channel is unavailable due to a communication issue

NGC 4151
Seyfert galaxy

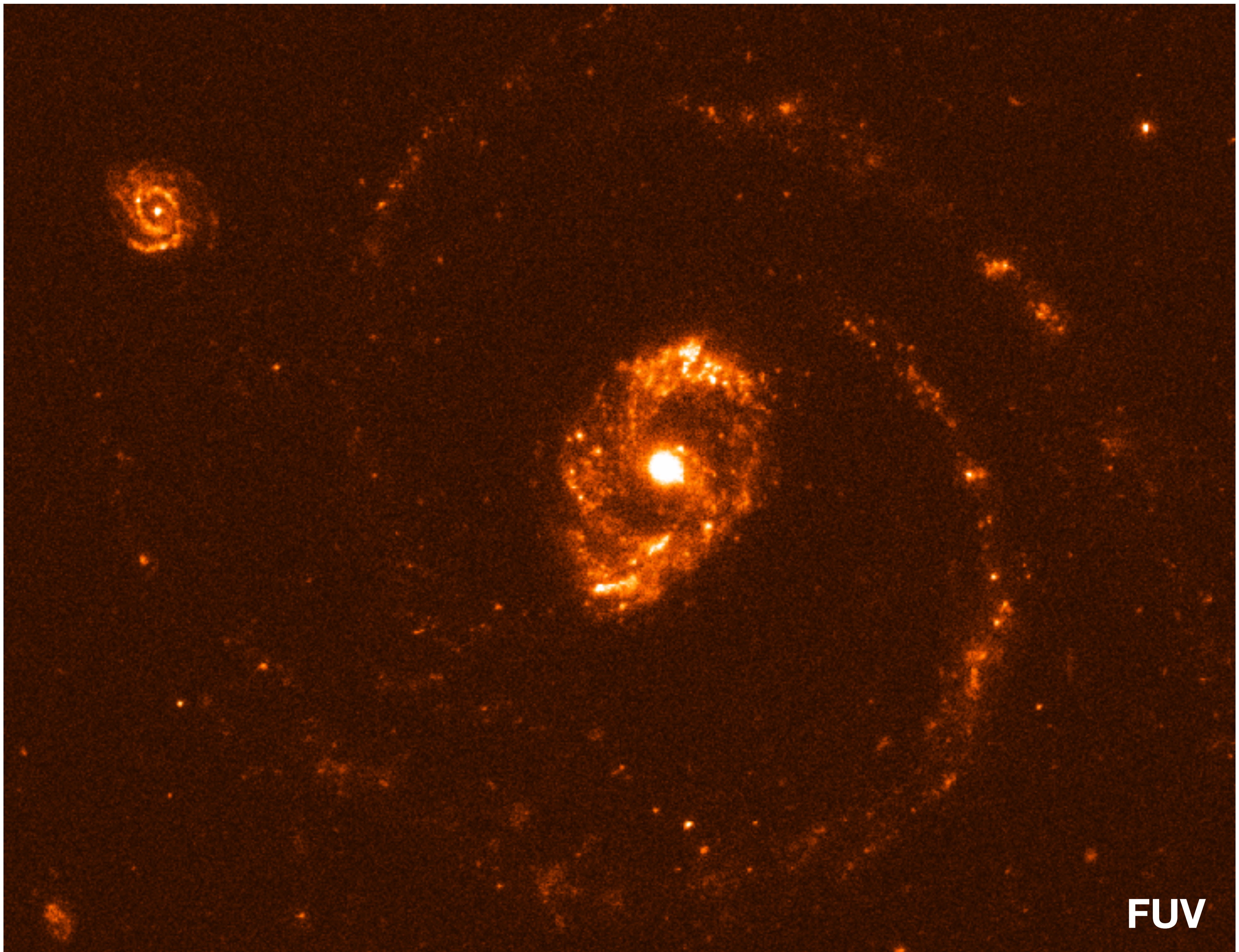

G.C. Dewangan et al

SXT on ASTROSAT

0.3 – 8 keV
A_{eff} ~ 120 cm^2 @ 1 keV
$E/\Delta E$ ~ 20 to 50

FOV ~ 40 arcmin

resolution ~ 3 arcmin

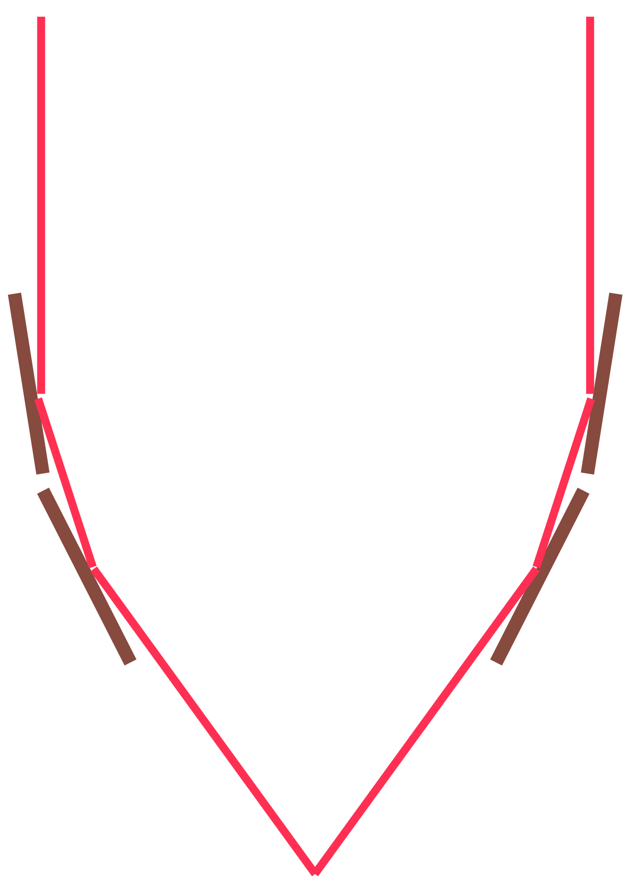

Built at TIFR, Mumbai and Univ. of Leicester

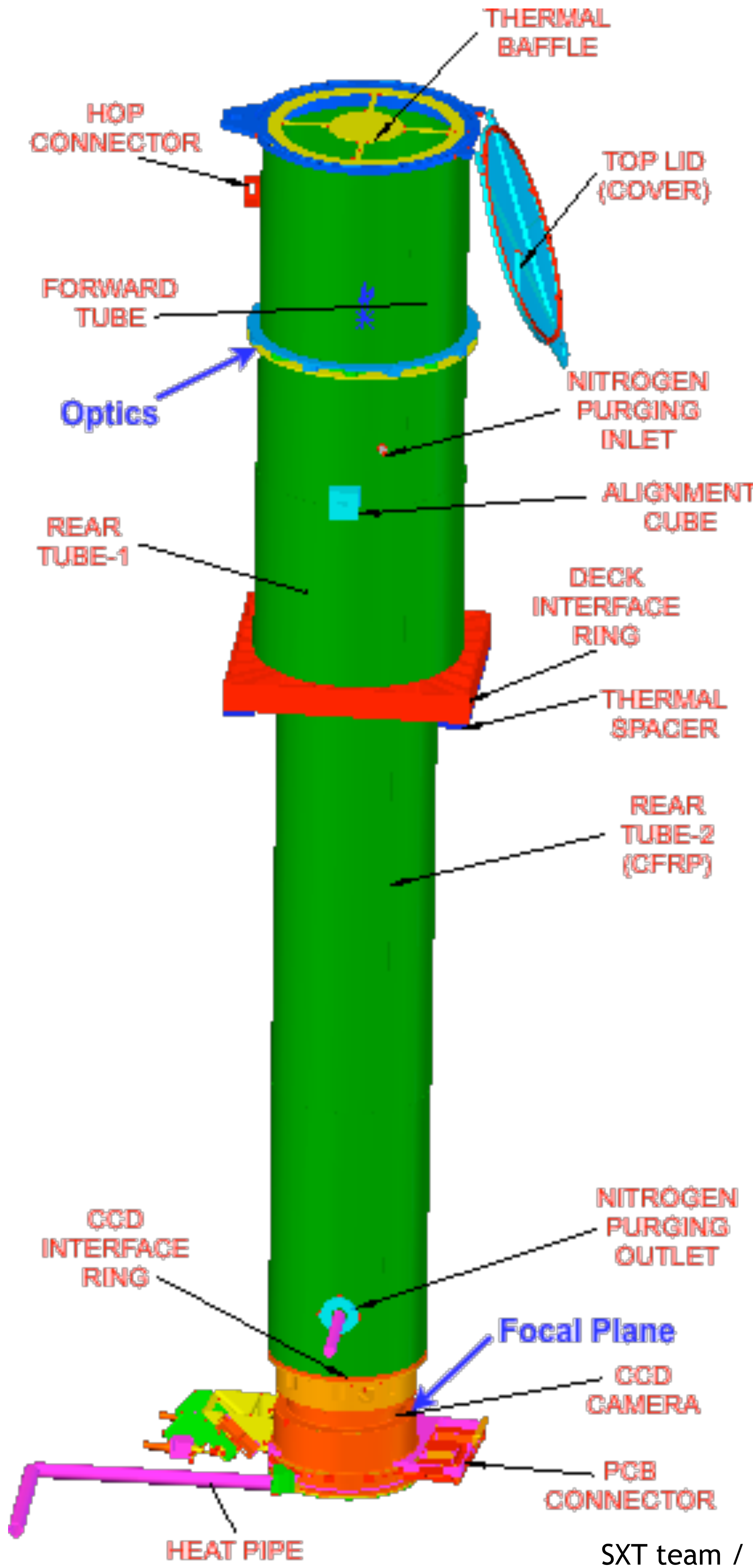

SXT team / K P Singh

Gold coated foil mirrors

Mirrors: Nested & Segmented conical surfaces in Wolter type I geometry working at Grazing incidence
39 nested shells

Spectroscopy with SXT

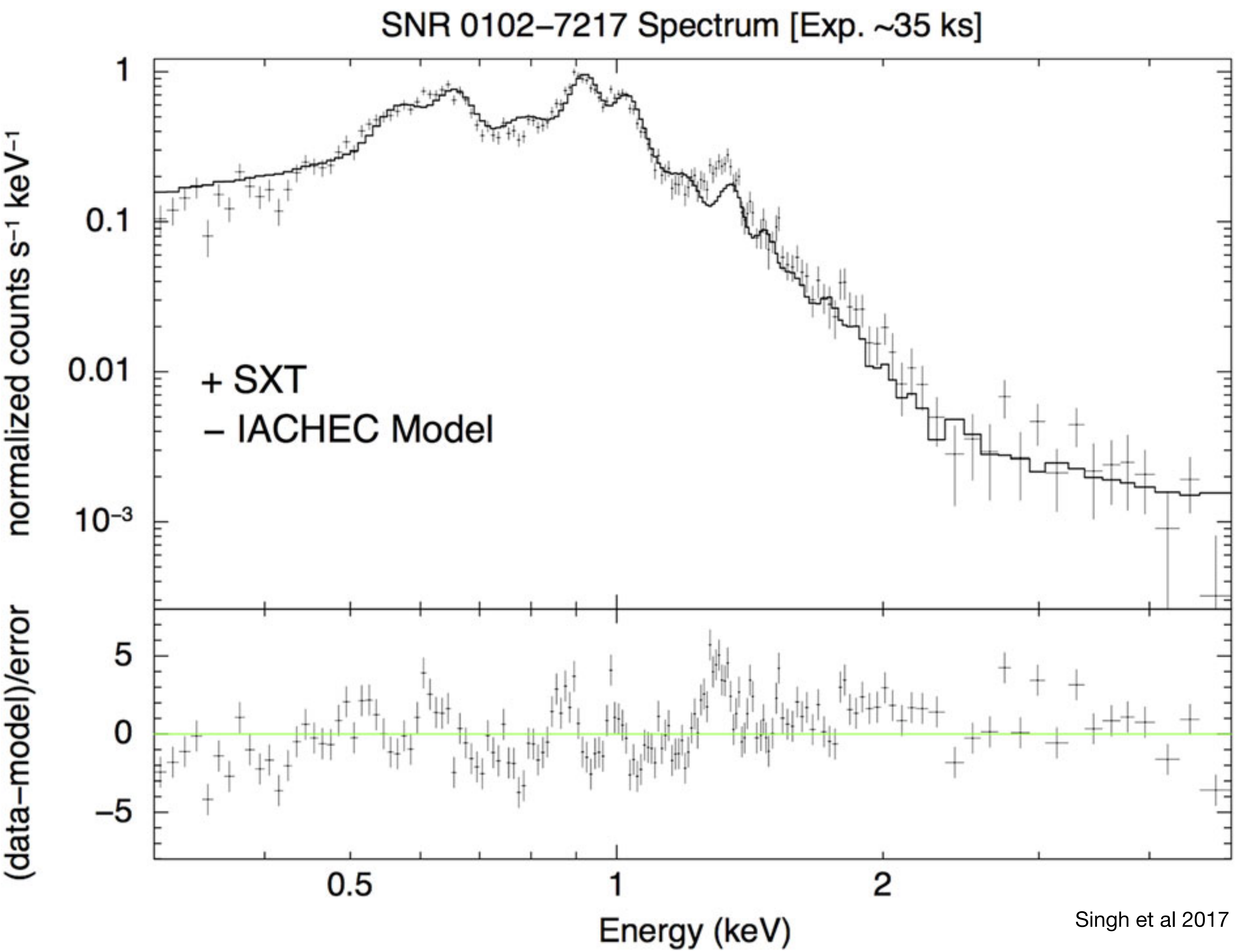

Singh et al 2017

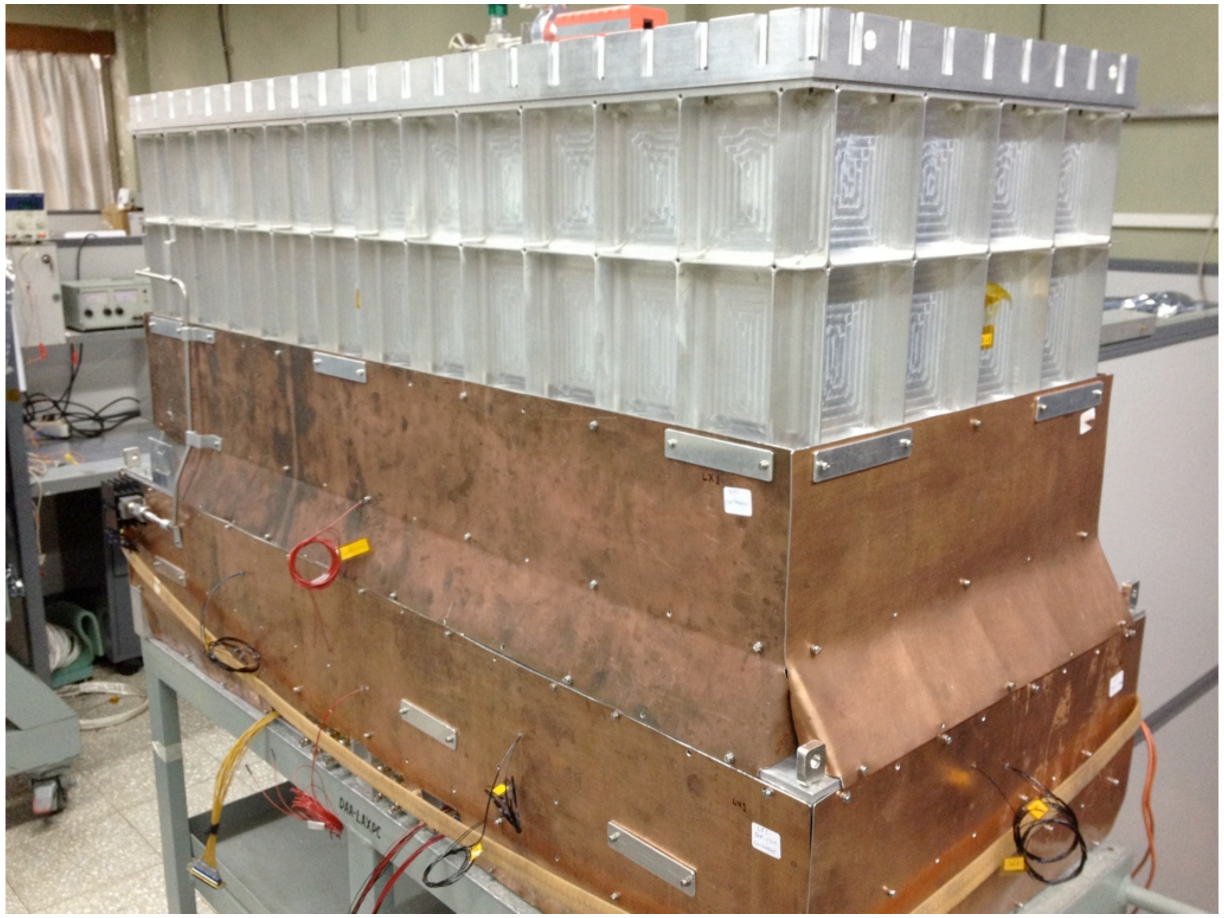

LAXPC team / J S Yadav

Large Area X-ray Proportional Counter (LAXPC) on AstroSat

3 units

3-80 keV

Energy resolution ~12-20%

Timing resolution 10 μs

Non-imaging, collimator 1 deg x 1 deg

Effective area ~2100 cm^2 per detector

BHXRB MAXI J1535-571: Spectro-timing behaviour

Bhargava et al 2019

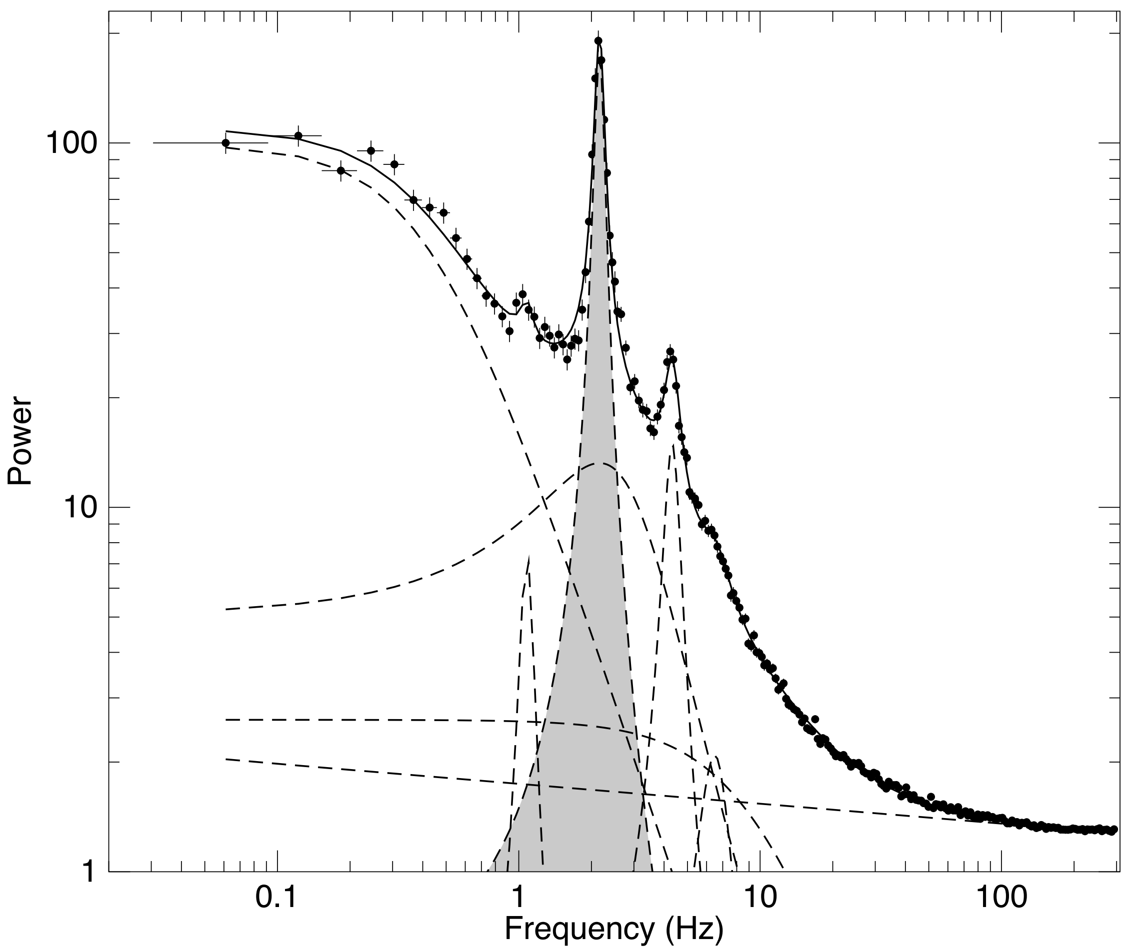

AstroSat LAXPC

Strong correlation between QPO frequency and power-law spectral index

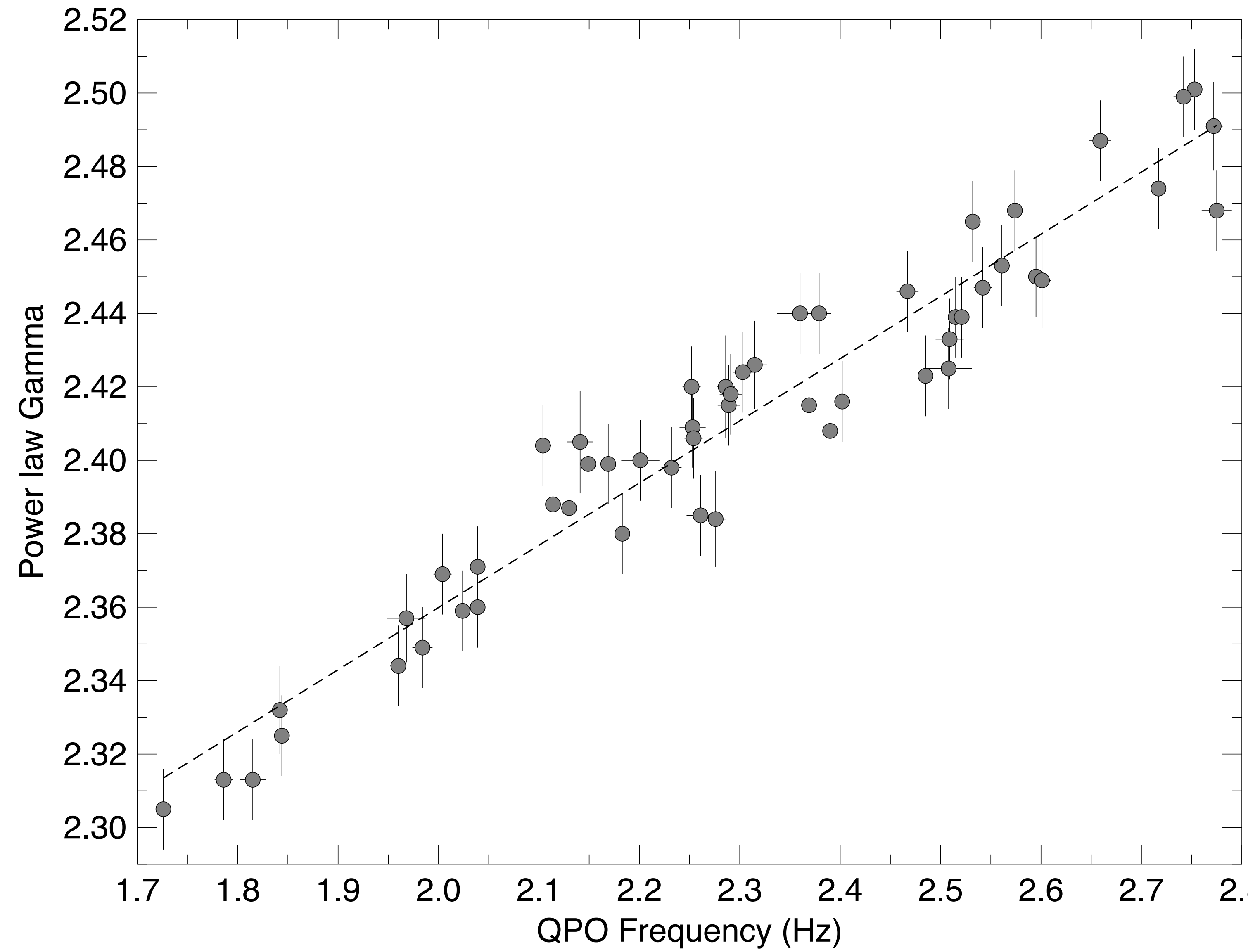

Oscillation arises in the Comptonising cloud

Crab Pulsar with AstroSat

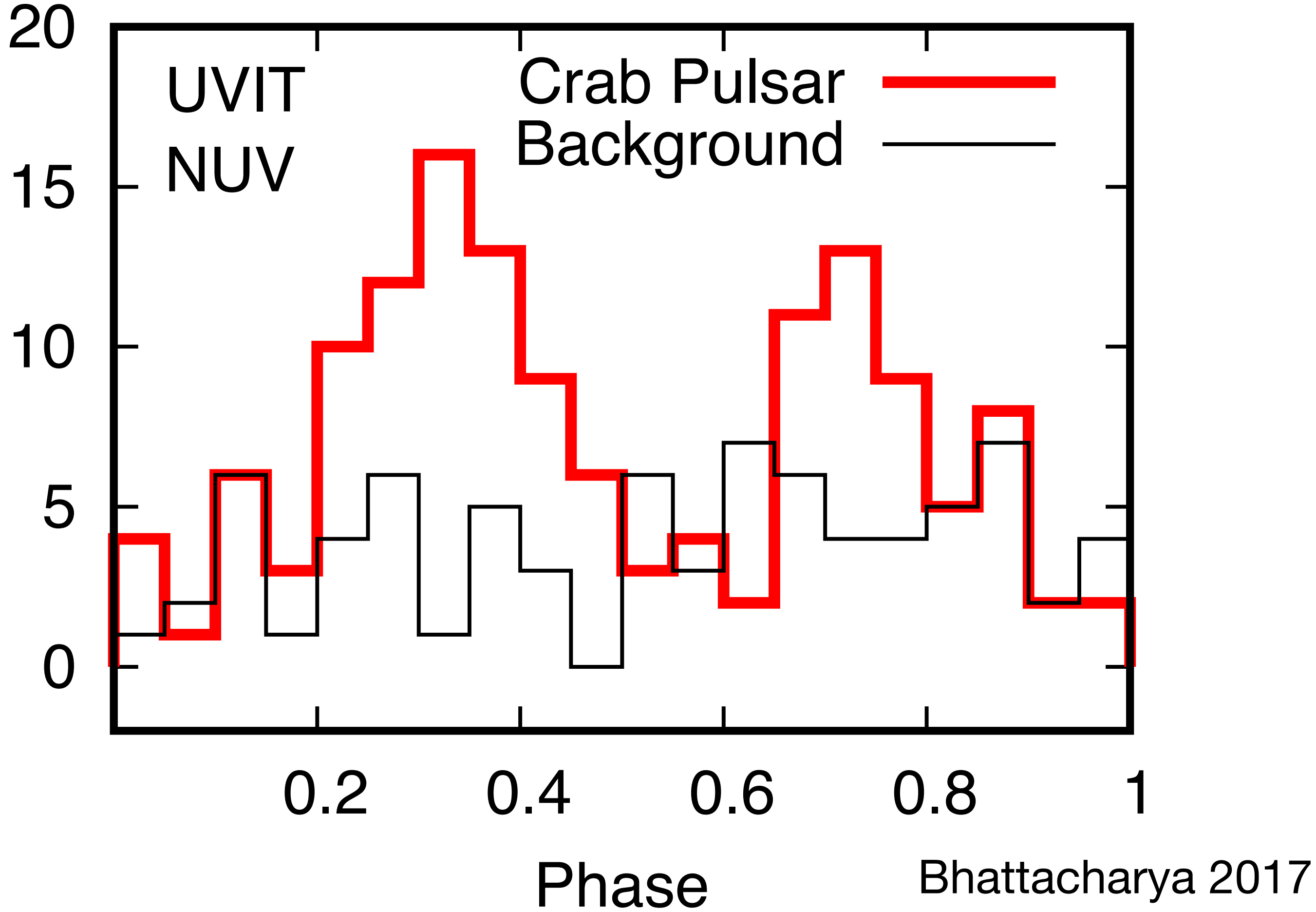

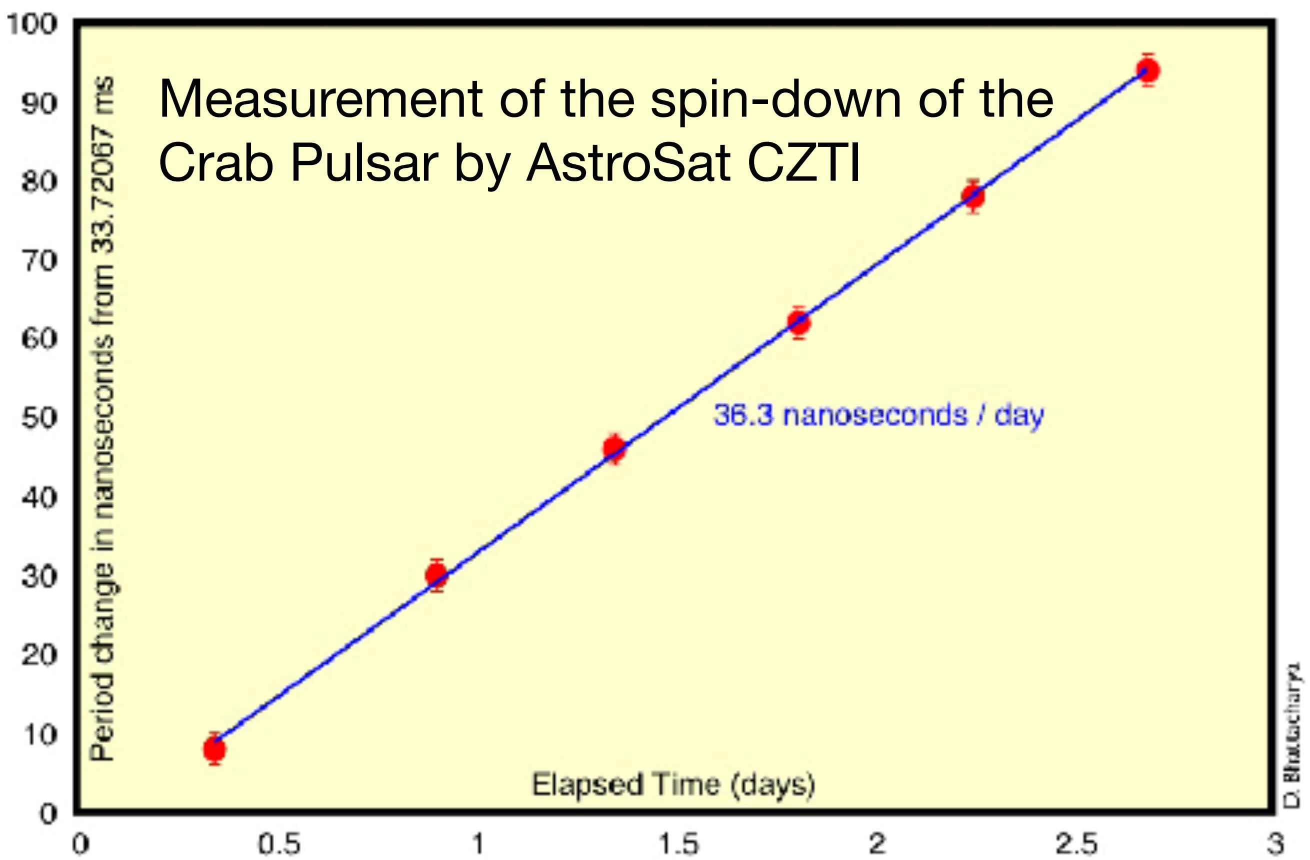

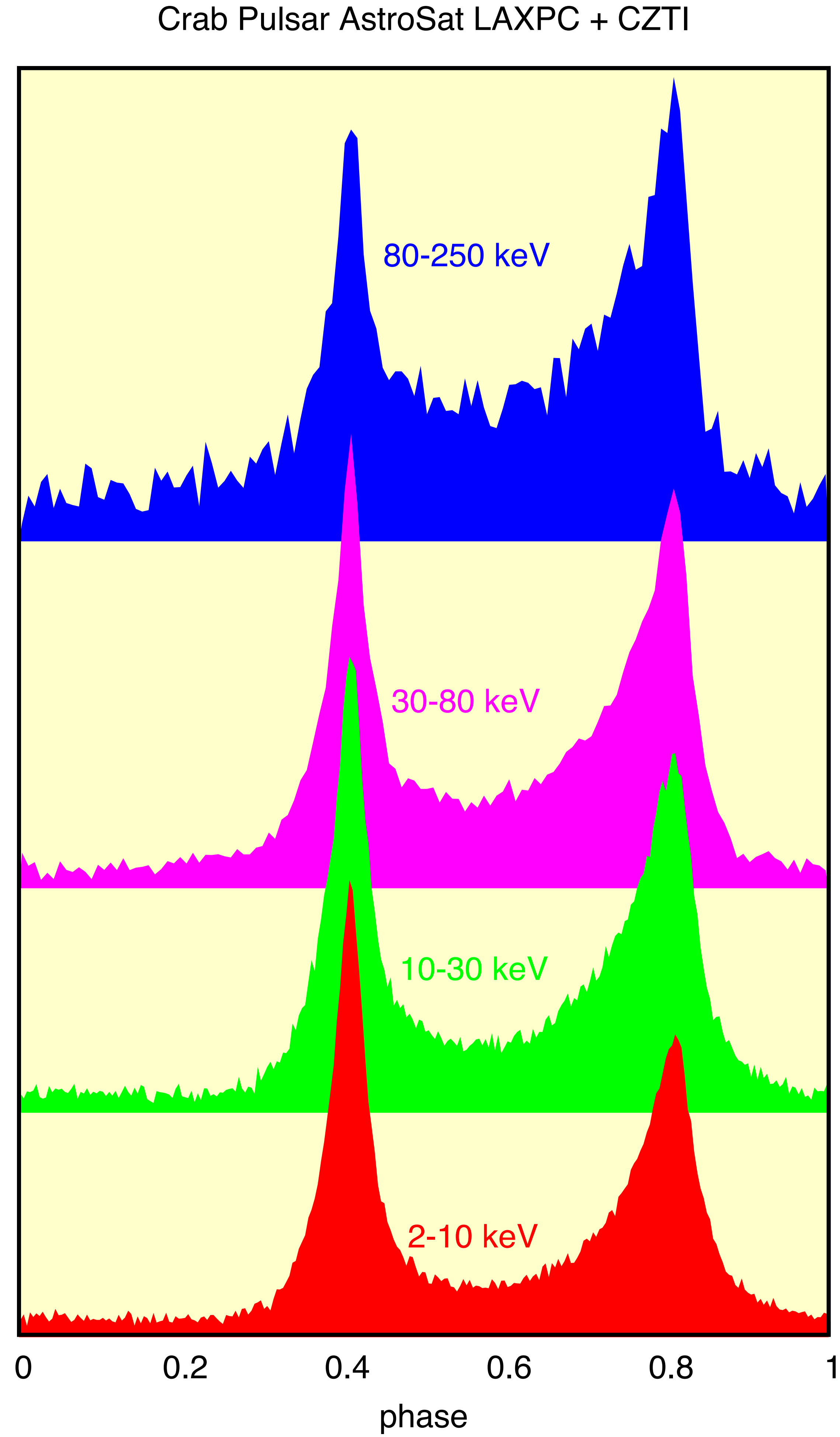

ASTROSAT Cadmium Zinc Telluride Imager

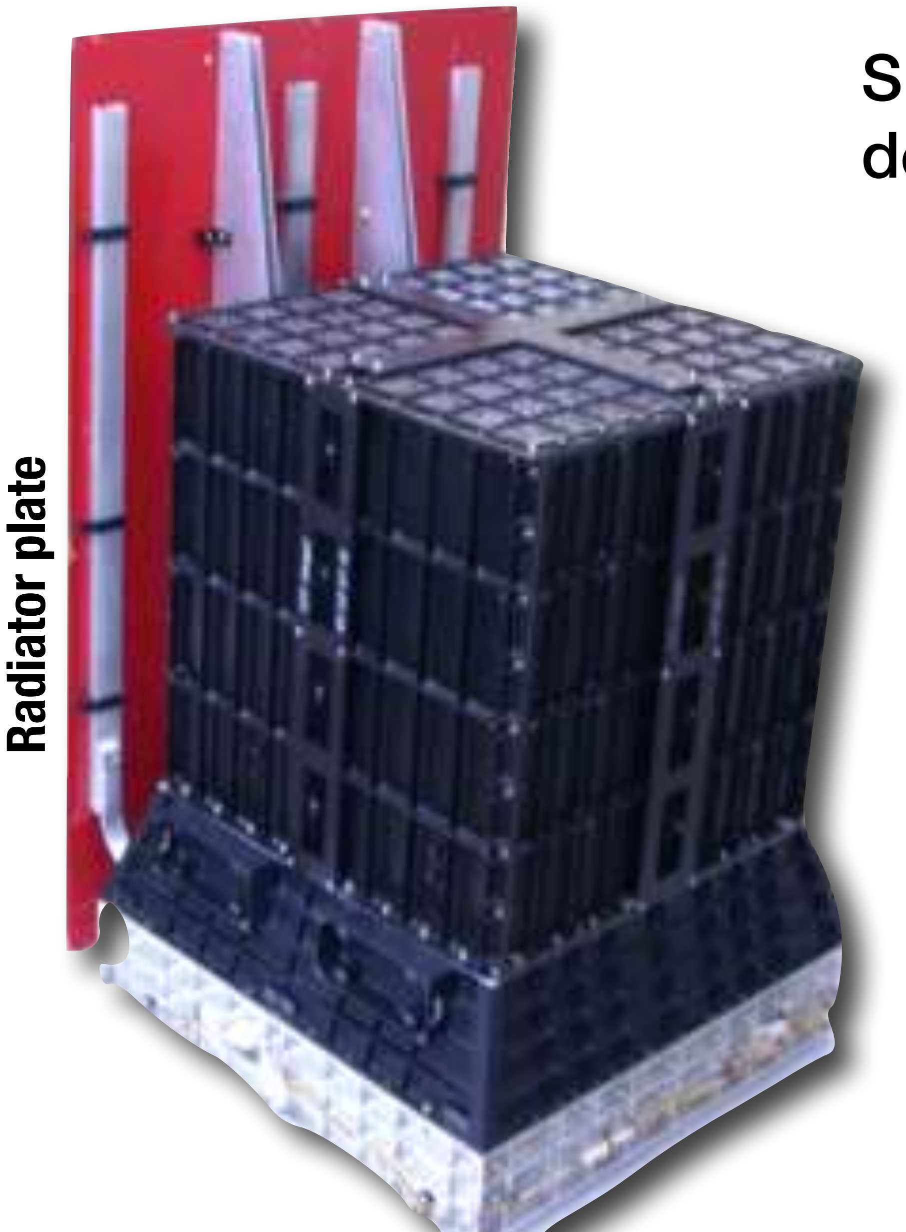

CZTI team / A R Rao

Cadmium-Zinc Telluride
is a high band gap (~2 eV)
semiconductor

Suitable for X-ray/γ-ray
detection

5mm thick CZT
2.5 mm pixels
256 pixels/module
16 modules/quadrant
Four quadrants

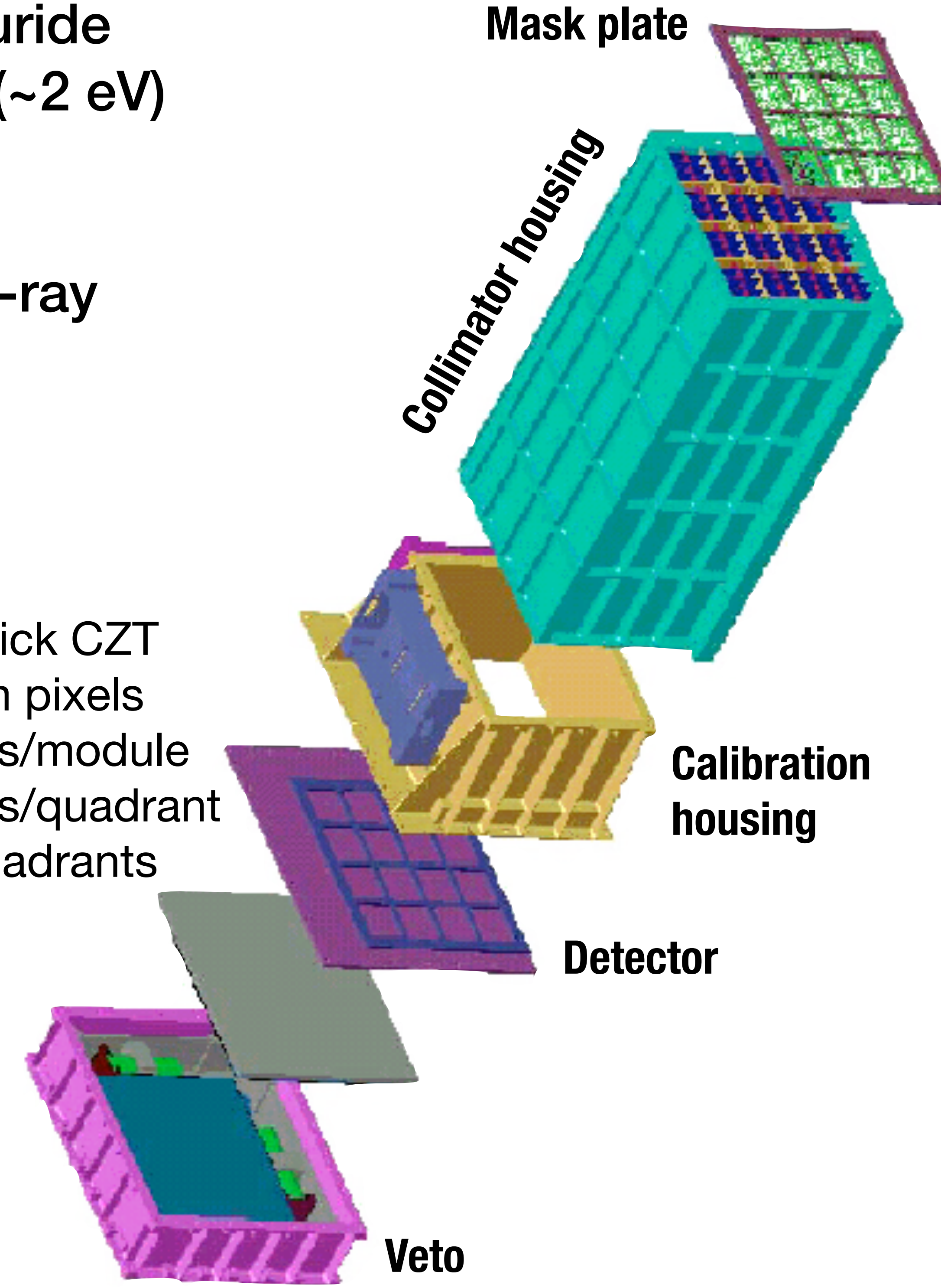

Built at TIFR, Mumbai and VSSC, Thiruvananthapuram

CZTI team / A R Rao

Cadmium-Zinc Telluride Imager (CZTI) aboard AstroSat

Geometric detector area 952 cm^2

Coded mask, 50% transmission
Collimators 4.6 deg x 4.6 deg

Energy resolution ~5%

Timing resolution 20 μs

Compton Polarimetry possible above 100 keV

CsI Veto detector below CZT detectors

Both CZT and Veto record GRB events

Am^{241} alpha-tagged calibration source at each quadrant

Astrosat CZTI mask design

Designed to gather as much independent information as possible

based on 256-element pseudo-noise Hadamard sets

16x16 elements per module

4x4 modules per quadrant
7 basic patterns, shuffled

4 quadrants
rotated patterns

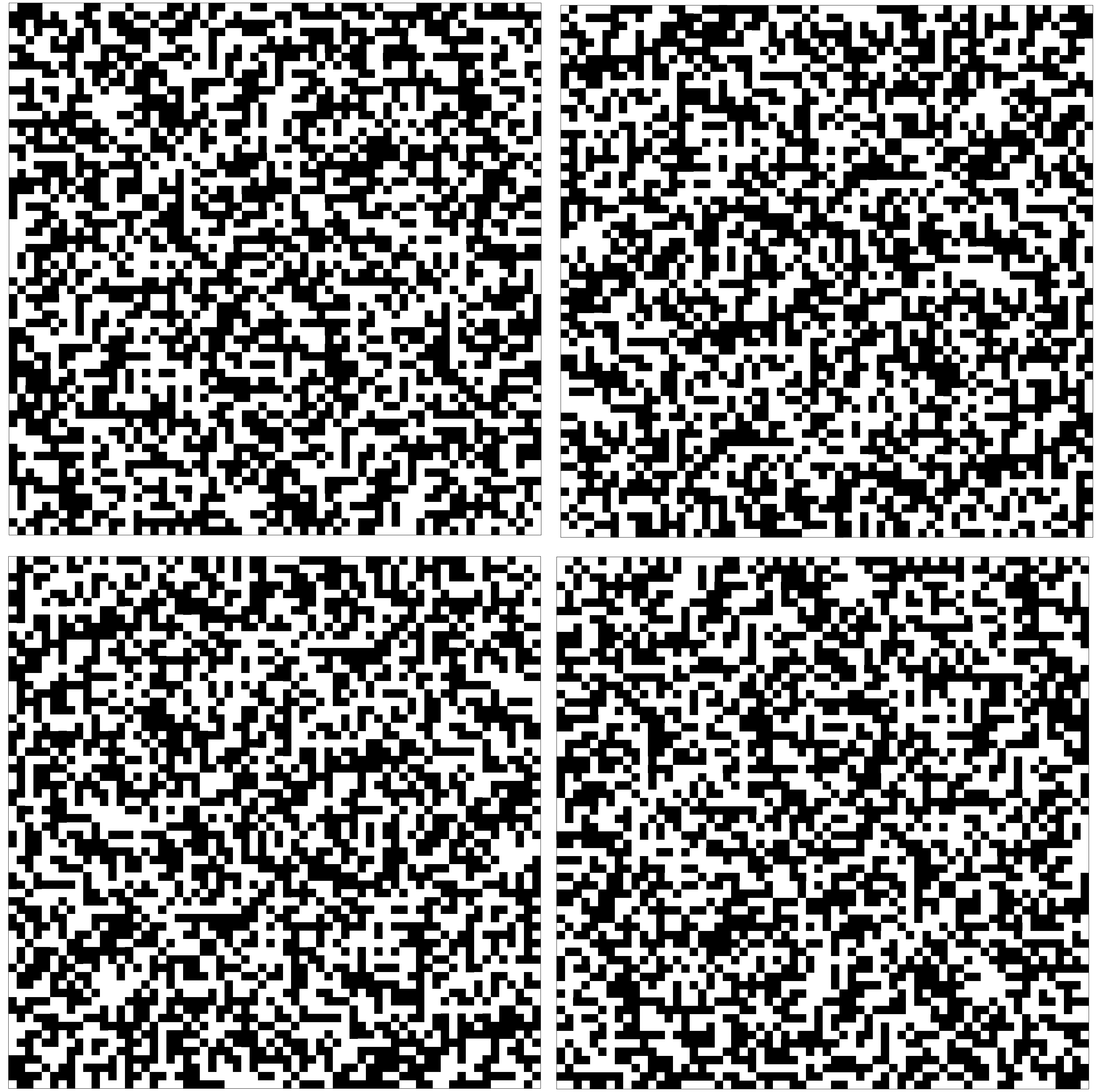

Black regions represent holes to be cut into the mask plate

Actual Fabricated Pattern for one quadrant.

Other quadrants have rotated versions

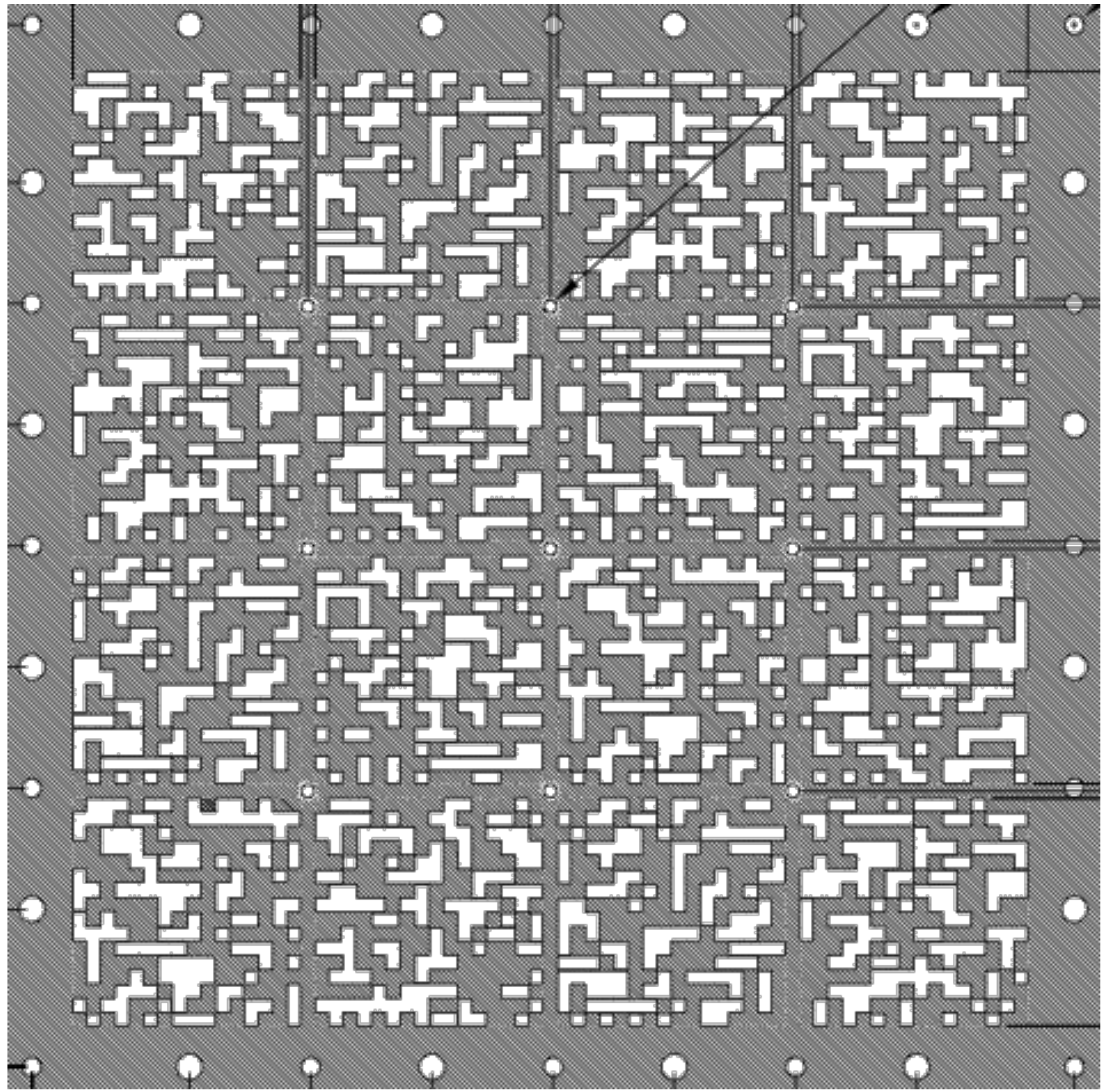

Mask of the same size as detector, elements the size of pixels

CZTI as a Hard X-ray Polarimeter
(100-380 keV)

Compton Polarimetry

$$\frac{d\sigma}{d\Omega} = \frac{3\sigma_T}{16\pi}\left(\frac{\omega'}{\omega_0}\right)^2\left(\frac{\omega_0}{\omega'} + \frac{\omega'}{\omega_0} - 2\sin^2\theta\cos^2\eta\right)$$

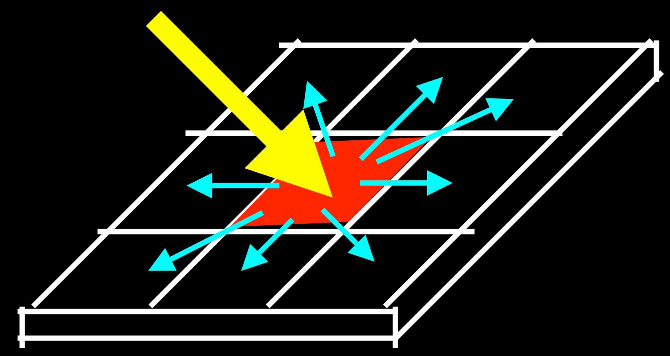

Distribution of azimuthal scattering angle η is measured

count rate $C(\eta) = A + B\cos^2(\eta - \phi)$

B = polarisation degree

ϕ = incident polarisation angle

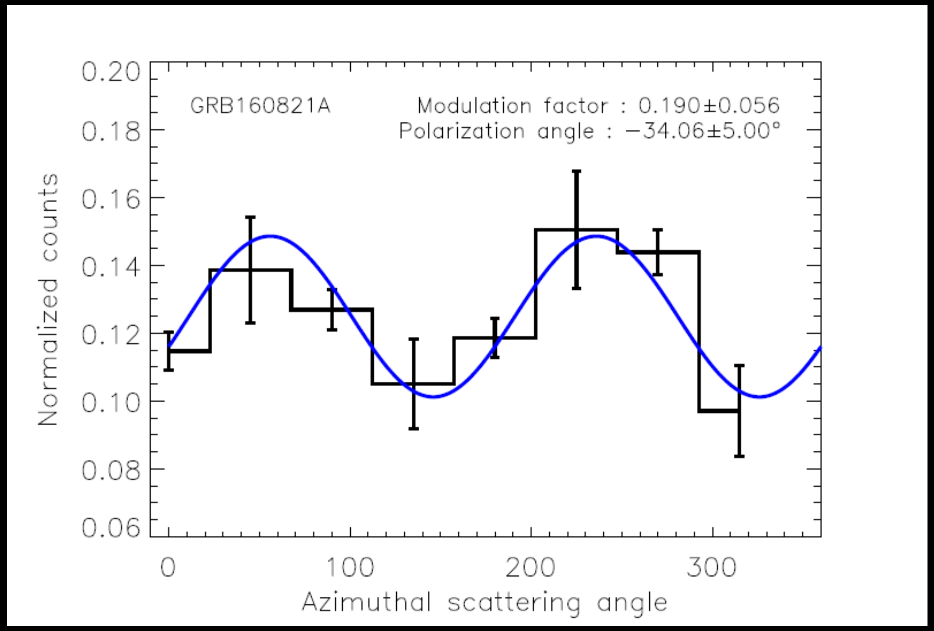

CZT Imager coordinate system

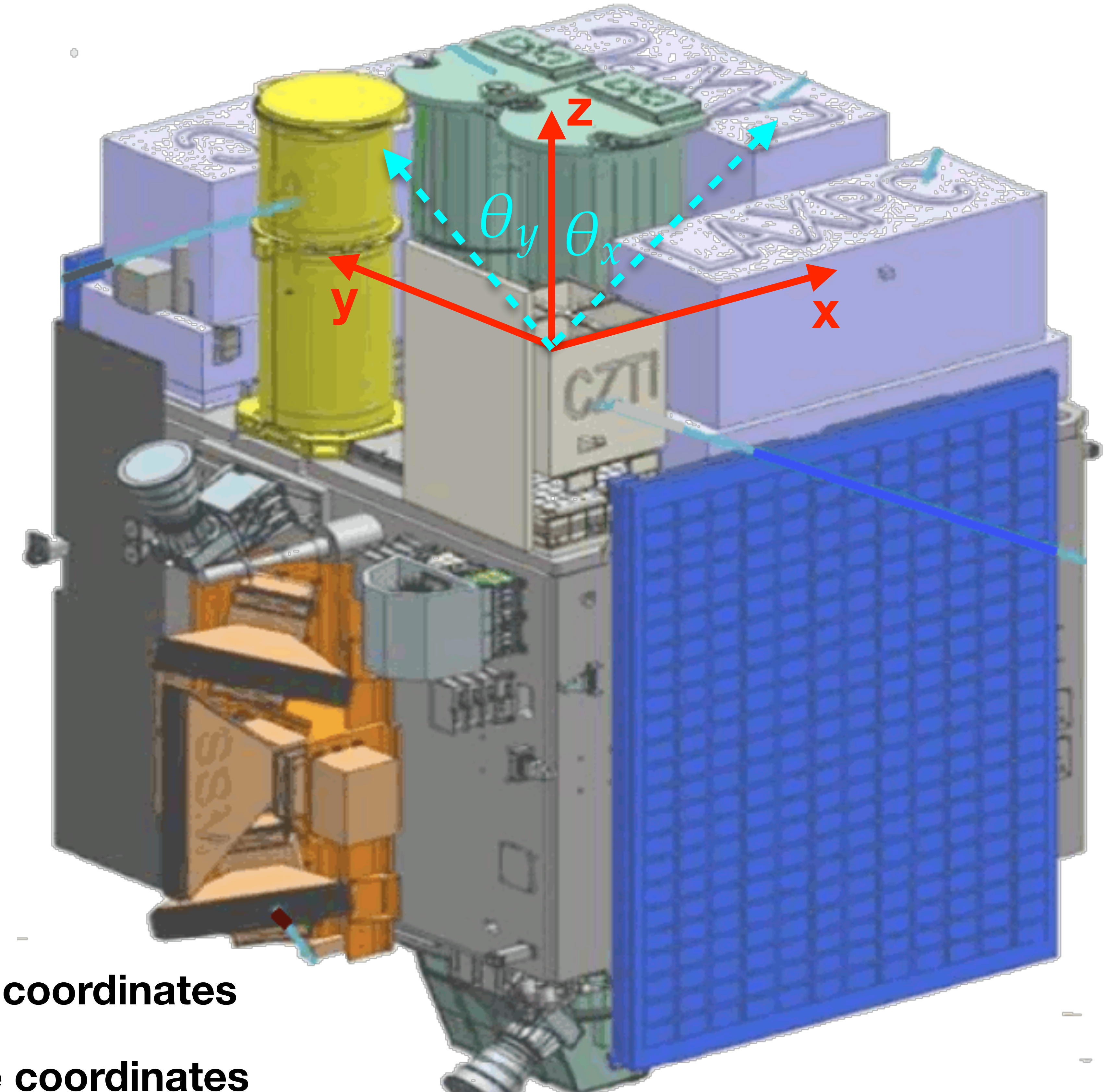

x,y,z: detector coordinates

θ_x, θ_y **: source coordinates**

CZTI data flow

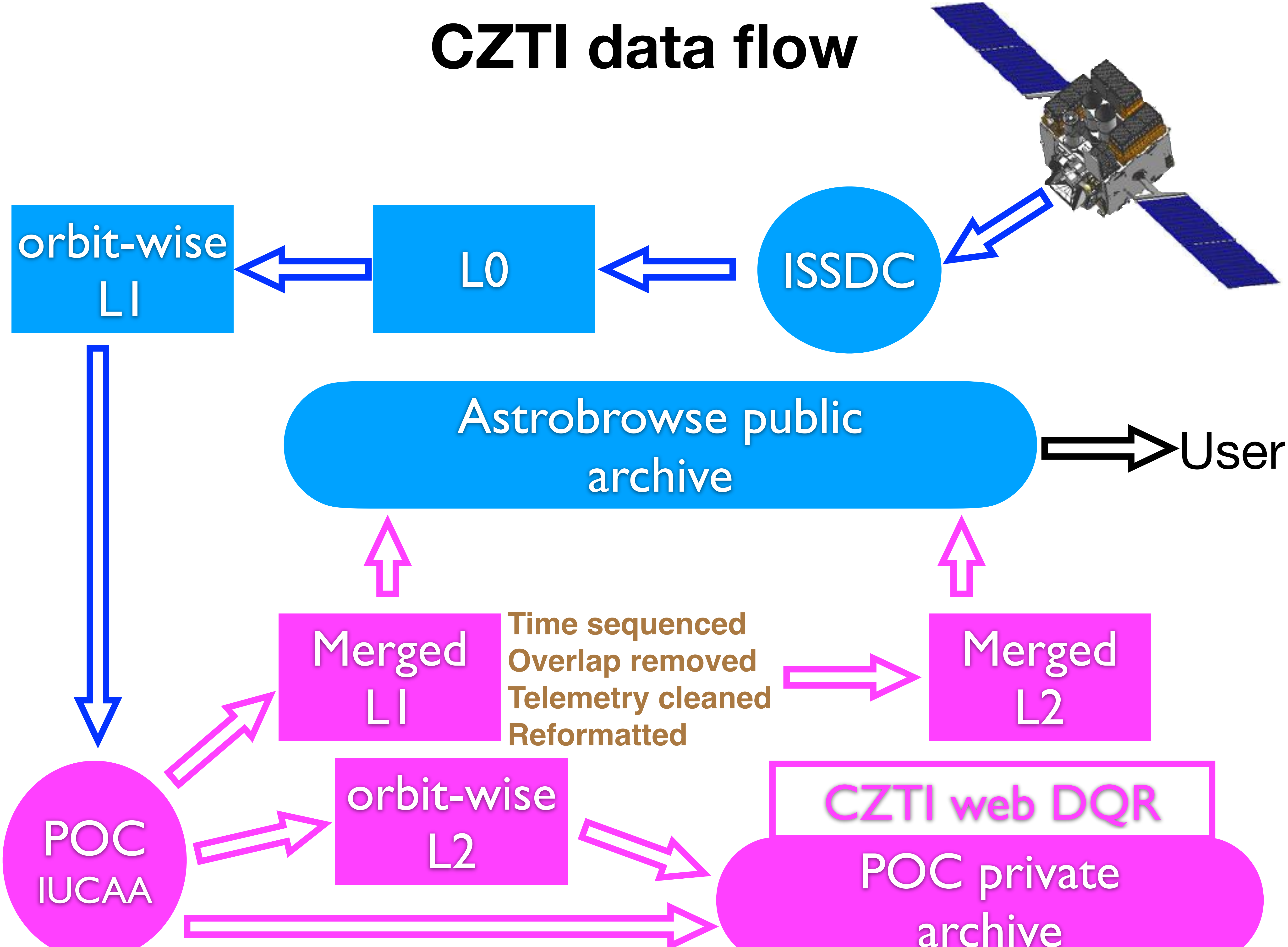

CZTI DQR page provides a quick summary of observations

http://www.iucaa.in/~astrosat/czti_dqr

ASTROSAT CZTI

Orbit-wise Data Quality Report

Last updated on: 2017-12-21T11:27:29.792969

Switch to: Orbit-wise | Merged OBSID-wise | Merged processing logs | Problem pages | Pixel enable/disable history | Module threshold history

Click on any table heading to sort by that column

Show 100 entries

Search:

Folder	OBSID	Observer	Object	RA	Dec	Exposure time	Date/time start	Date/time end
20170827_G07_048T01_9000001494_level2_10357	NA	NA	NA	NA	NA	NA	NA	NA
20171221_A04_176T01_9000001786_level2_12062	A04_176T01_9000001786	KshamaSK	NGC 2685	133.8942	58.73444	3462.80067128	2017-12-21 01:26:38	2017-12-21 02:57:34
20171219_A03_085T02_9000001784_level2_12062	A03_085T02_9000001784	pbera	1RXS J032540.0-081442	51.41657	-8.245	5386.73443553	2017-12-20 22:38:43	2017-12-21 01:02:27
20171219_A03_085T02_9000001784_level2_12060	A03_085T02_9000001784	pbera	1RXS J032540.0-081442	51.41657	-8.245	4907.69821505	2017-12-20 21:03:15	2017-12-20 23:24:36
20171219_A03_085T02_9000001784_level2_12059	A03_085T02_9000001784	pbera	1RXS J032540.0-081442	51.41657	-8.245	4309.54354214	2017-12-20 19:29:55	2017-12-20 21:37:17
[illegible]	A03_085T02	[illegible]	1RXS	[illegible]	[illegible]	4412.42538	2017-12-20	2017-12-20

CZTI Level1-2 data analysis pipeline

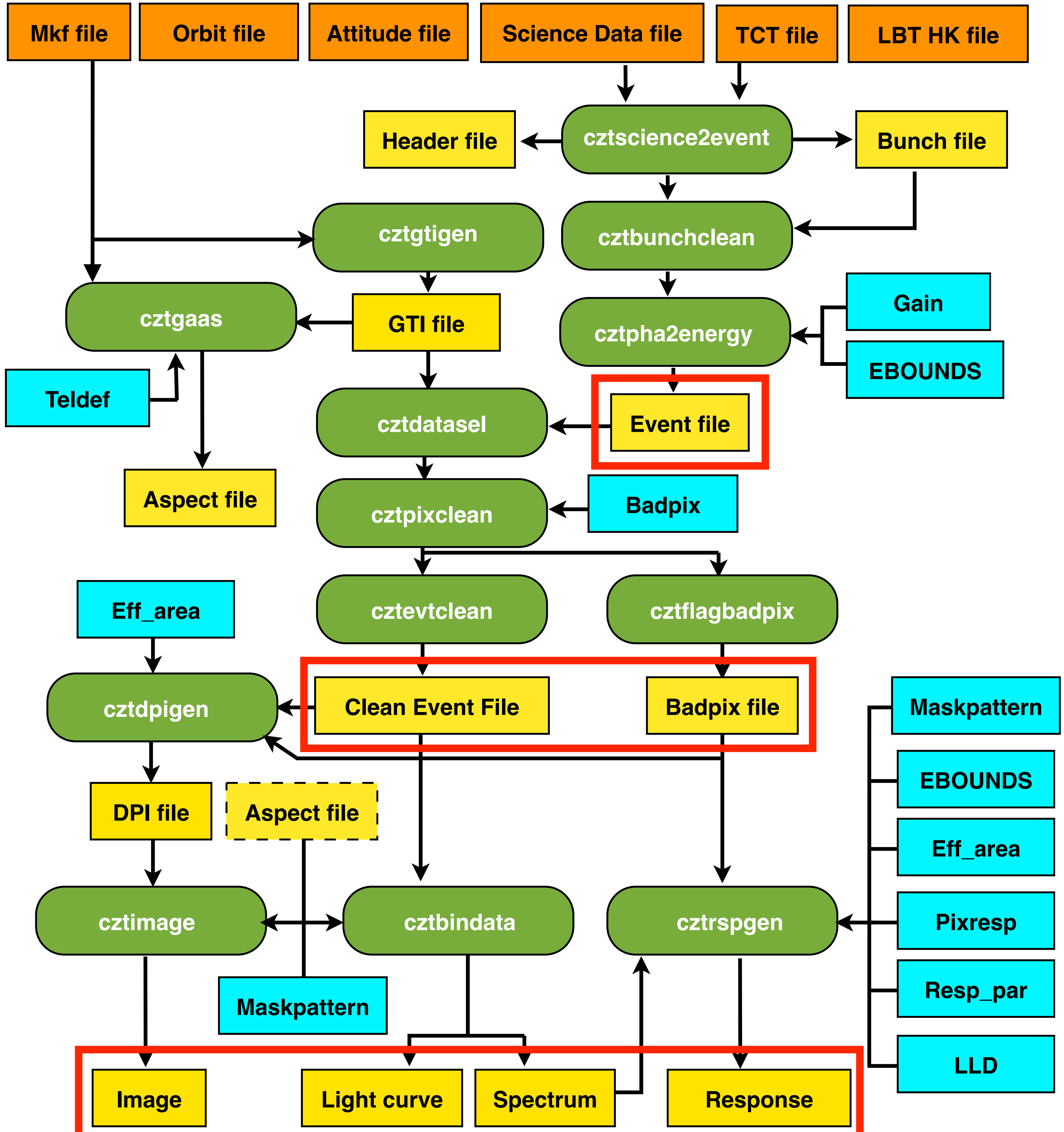

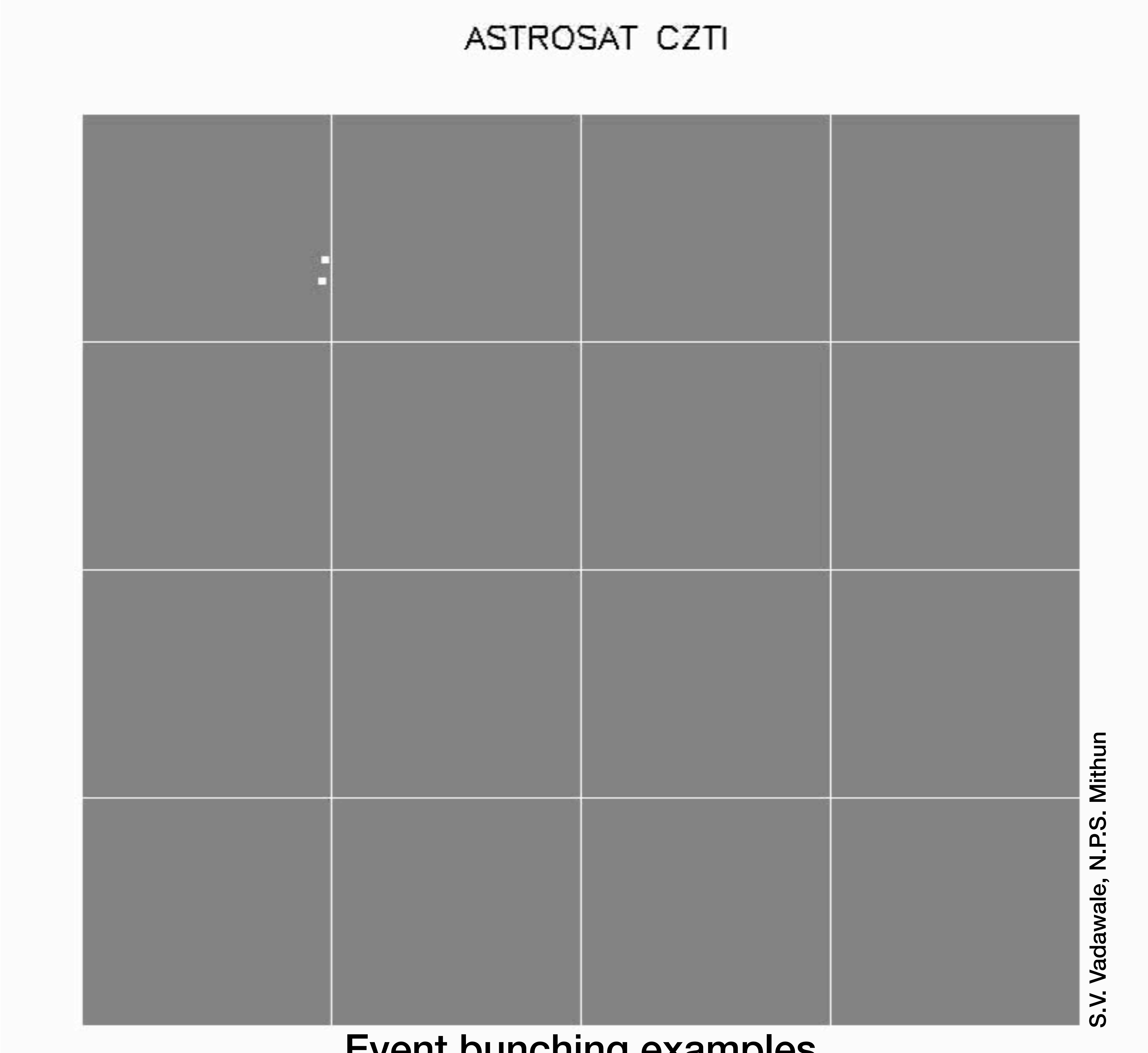

Event bunching examples

Pixel selection

- Grade: dynamically determined + CALDB
- Grade 0 = good, 1 = spectroscopically bad, 2 = flickering, 3 = noisy, 4 = dead
- Grade 2-4 : ~ 8%
- Grade 1 : ~20% (can be used for imaging and timing but not for spectroscopic work)
- CALDB has detailed response function for each of the 16384 pixels. Used for generating combined weighted response

A_{geom} ~ 976 cm^2 ~50% blocked by CAM

A_{eff} for spectroscopy ~ 340 cm^2 @ 30-100 keV

Making an image

Start with an event file

Count the number of events occurring in each pixel, creating a Detector Plane Histogram (DPH)

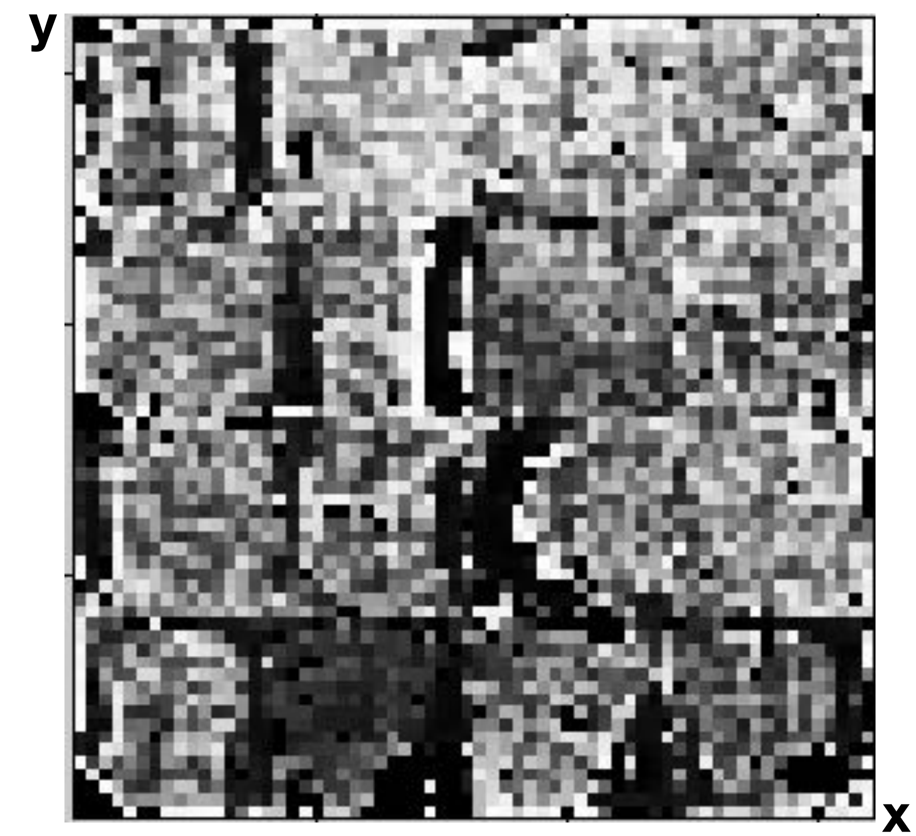

Quadrant Q0, ObsID 1694

Normalise the DPH count in each pixel by the relative effective area of the pixel. This yields a Detector Plane Image (DPI)

D_i = DPI count in pixel i

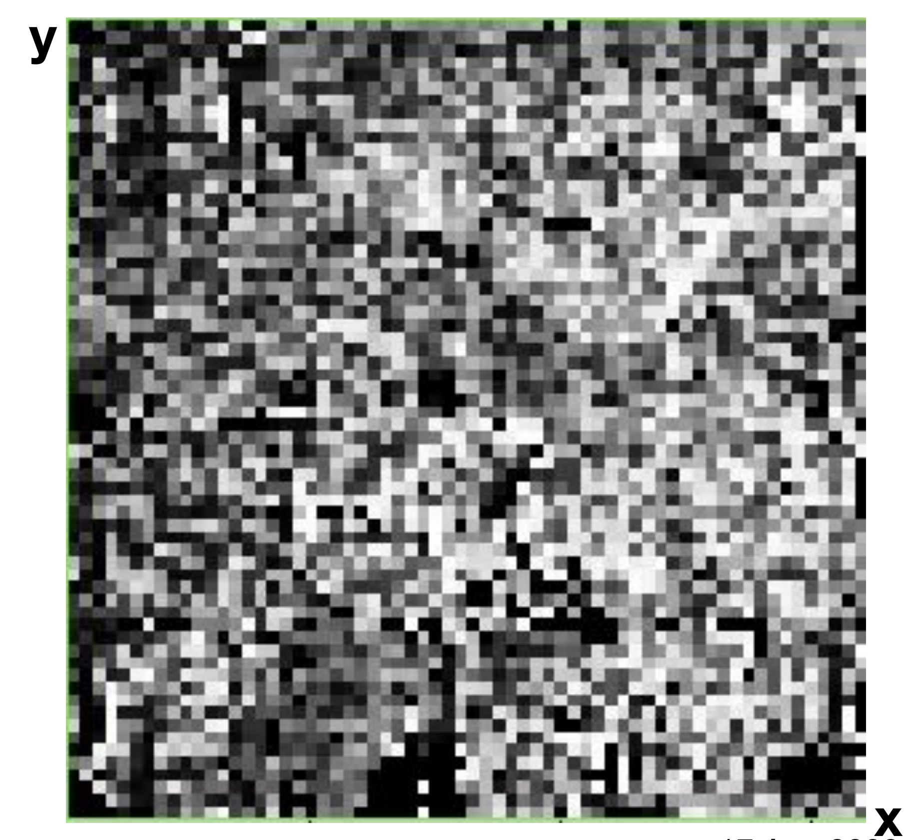

This is a linear combination of shadows cast by the sources in the FOV

Reconstructing the sky plane image

Quick Method

Look for a shifted replica of the mask pattern M_i

$\{M_i\}$ **is a collection of 0-s (closed) and 1-s (open)**

Cross correlate $\{M_i\}$ **and** $\{D_i\}$ **via FFT**

$$\{S_j\} = \mathcal{F}^{-1}[\mathcal{F}\{M_i\} \times \mathcal{F}\{D_i\}]$$

$\{S_j\}$ **is a collection of source intensities at sky elements** j

This is the imaging algorithm used in the pipeline software at present

Slight misalignments between the mask and the detector are accounted for by using a calibrated phase matrix $\{\phi_i\}$

$$\{S_j\} = \mathcal{F}^{-1}[\mathcal{F}\{M_i\} \times \{\phi_i\} \times \mathcal{F}\{D_i\}]$$

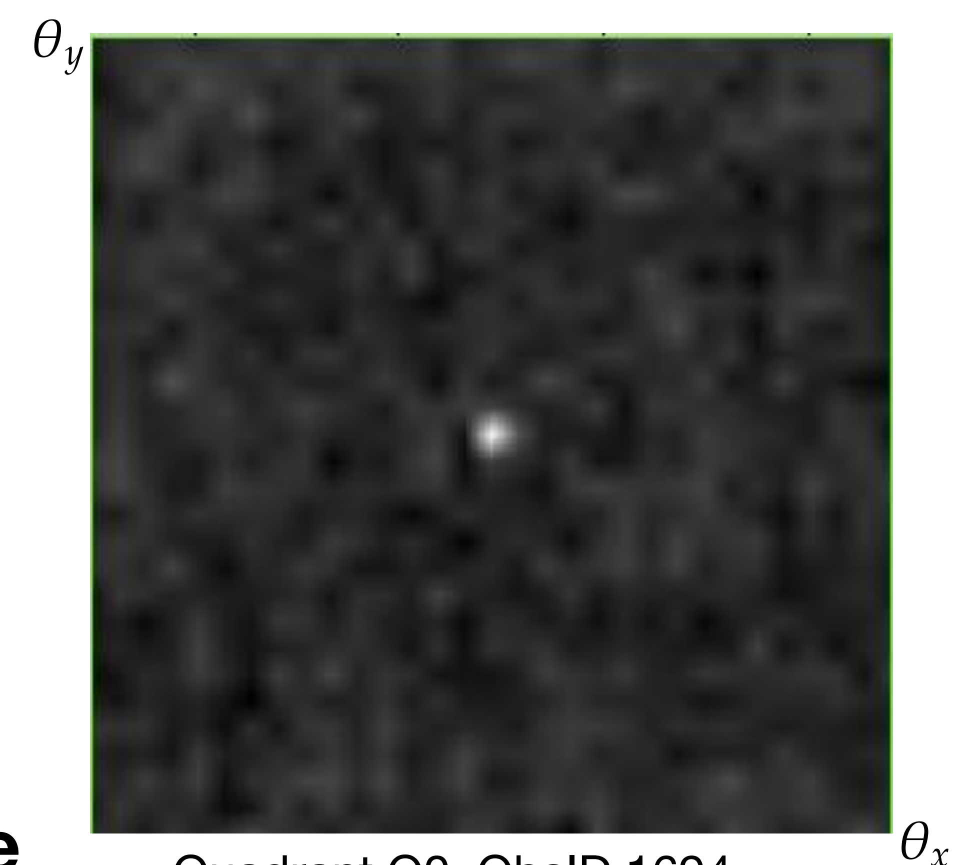

Quadrant Q0, ObsID 1694

Pro:
Computational economy

Con:
Does not account for partial shadowing of pixels, flux estimates inaccurate, higher coding noise

Reconstructing the sky plane image

More rigorous methods

Compute expected shadows of sources in different directions: $\{R_{ij}\}$
Use ray tracing, include all effects e.g. camera structure, partial transparency of mask plate, energy dependence etc.

$\{R_{ij}\}$ **can then be used in several ways**

Cross Correlation: $\{C_j\} = \{R_{ij}\} * \{D_i\}$

Balanced Cross Correlation: $\{\mathcal{S}_j\} = \{R_{ij}\} * \{D_i\}/N_o \; - \; \{\tilde{R}_{ij}\} * \{D_i\}/N_c$

Forward fitting: $D_i = \sum_j R_{ij} S_j$ **Fit** $\{S_j\}$ **to reproduce** $\{D_i\}$

Bayesian inference: $S_j^{(n+1)} = S_j^{(n)} \sum_i R_{ij} \frac{D_i}{\sum_j R_{ij} S_j^{(n)}}$ **Richardson-Lucy iterative reconstruction**

These algorithms have been implemented and tested with CZTI data. Some of them will be made available in future releases of the pipeline.

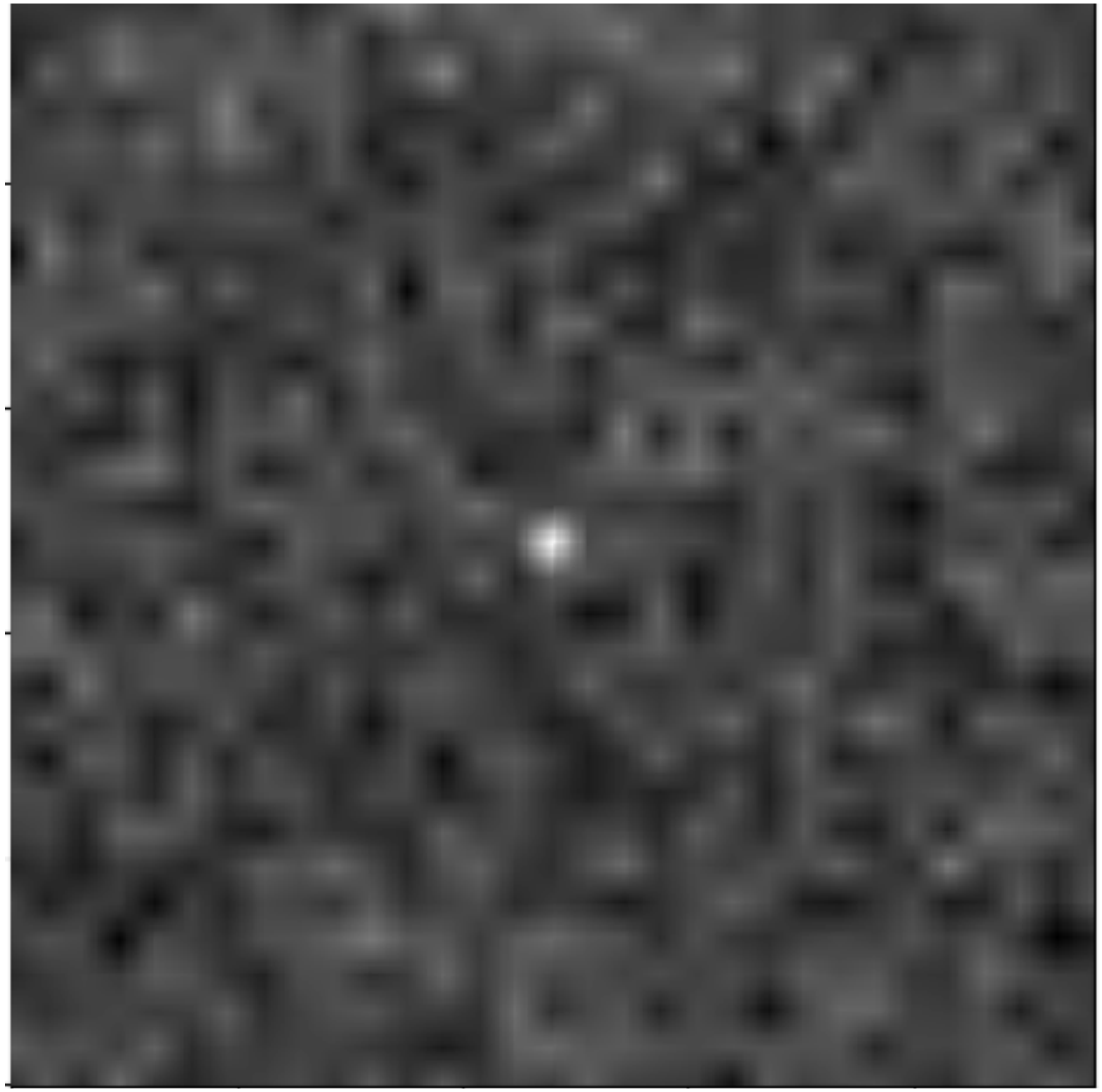

FFT image

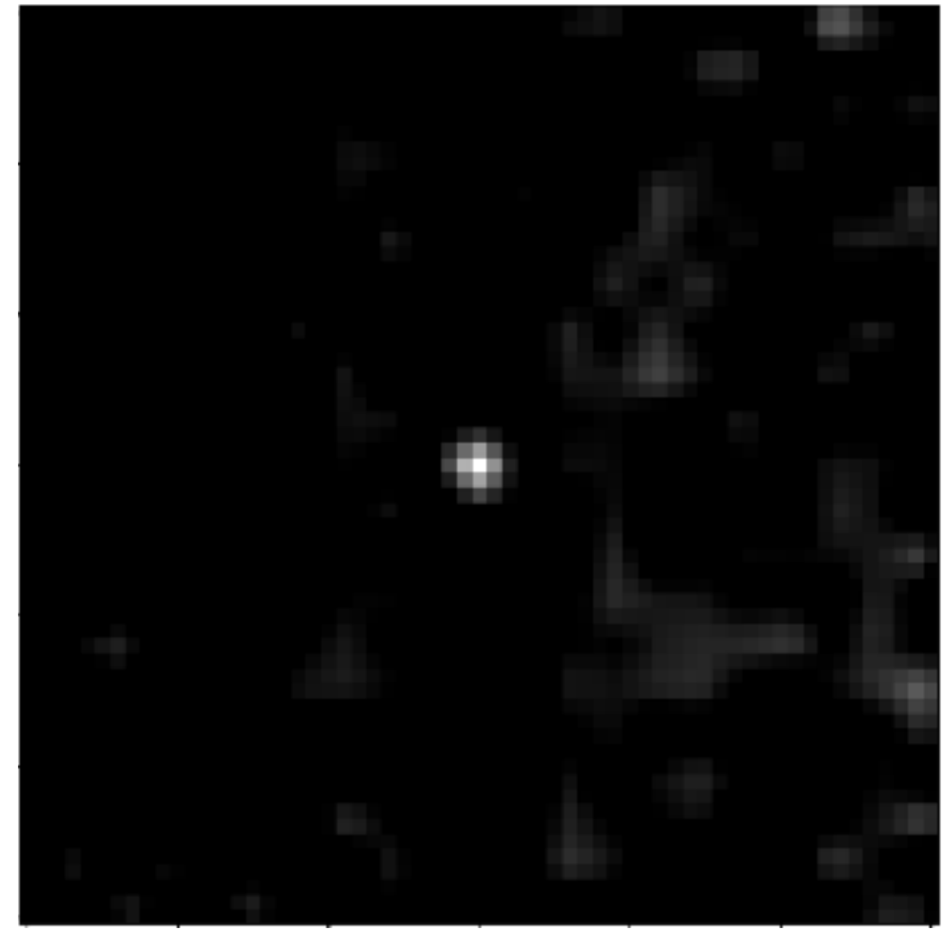

Cross correlation

Using $\{R_{ij}\}$

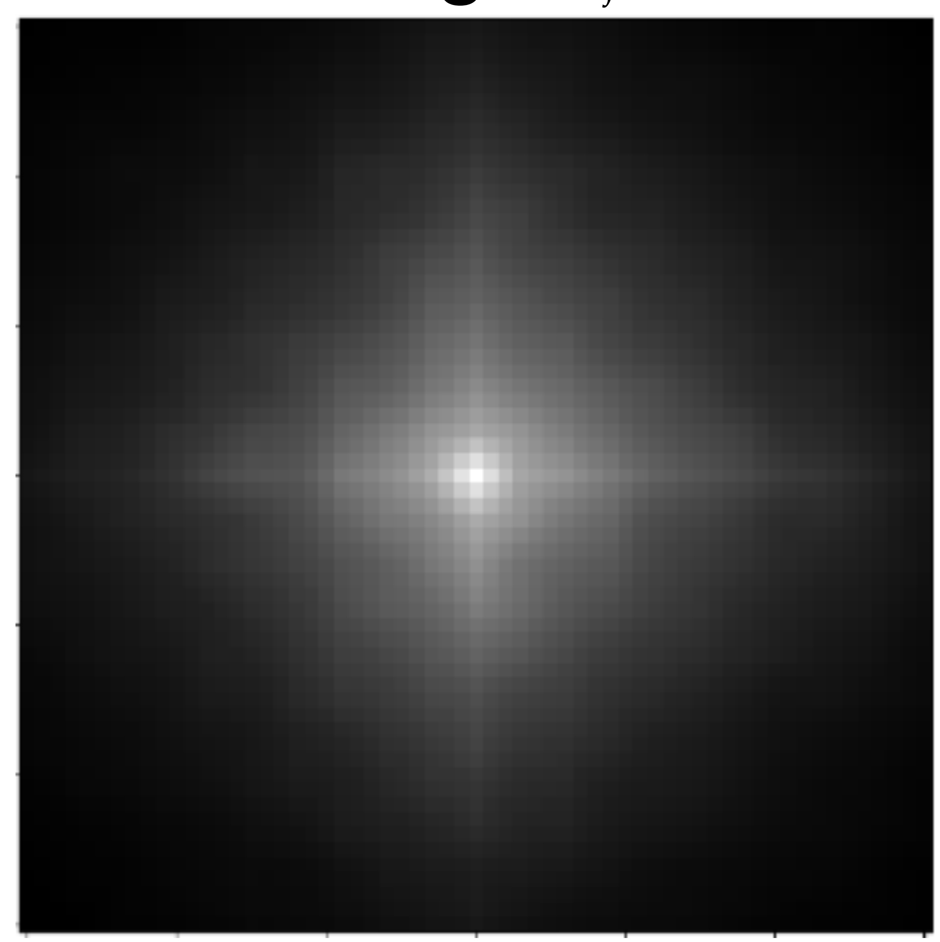

Richardson-Lucy

Vibhute et al 2017

Crab: extract from ObsID 406
duration 50 second

Quadrant Q0 only

Mask Weighting

Used to estimate background subtracted flux of a single dominant source at a known location in the FOV

For a given source location (θ_x, θ_y) **in camera coordinates, the fractional exposure** f_i **of pixel** i **can be computed by ray tracing.**

If S **is the source flux and** B **the background flux (counts/area) then**

DPH count $D_i = (f_i S + B)a_i$ **[** a_i **= pixel effective area]**

Define Mask Weight $w_i = (2f_i - \alpha)$ **such that** $\sum_i w_i a_i = 0$

Then $\sum_i w_i D_i = S \sum_i w_i f_i a_i$ **;** **Hence** $S = \dfrac{\sum_i w_i D_i}{\sum_i w_i f_i a_i}$

This can be done for different energy selections, generating a spectrum or for different time bins, yielding a light curve.

In CZTI pipeline, mask weighting estimate is done separately for every second of data in order to compensate for pointing jitter.

Crab, Q0, ObsID 406

Mask weighted spectrum

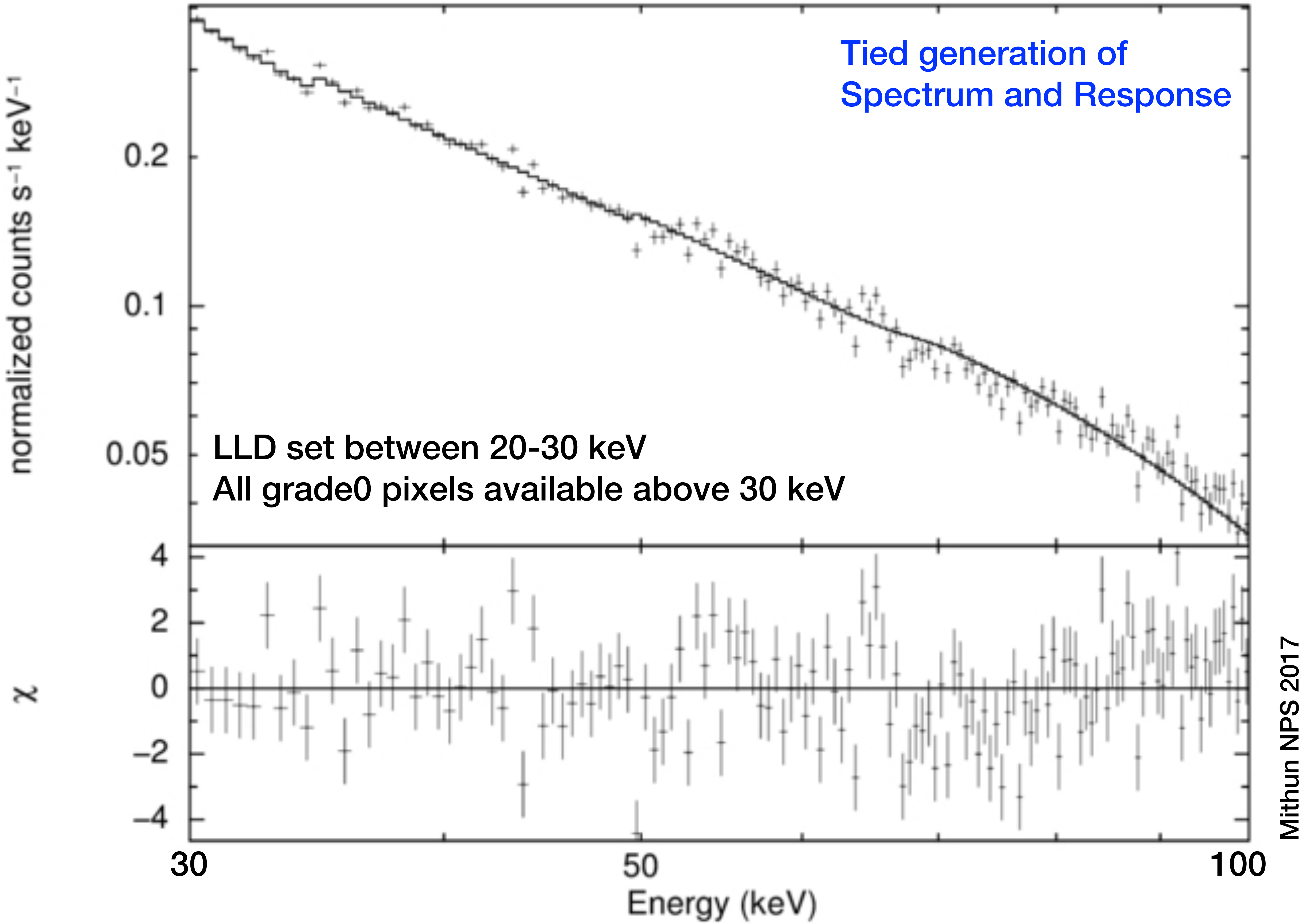

Timing with CZTI

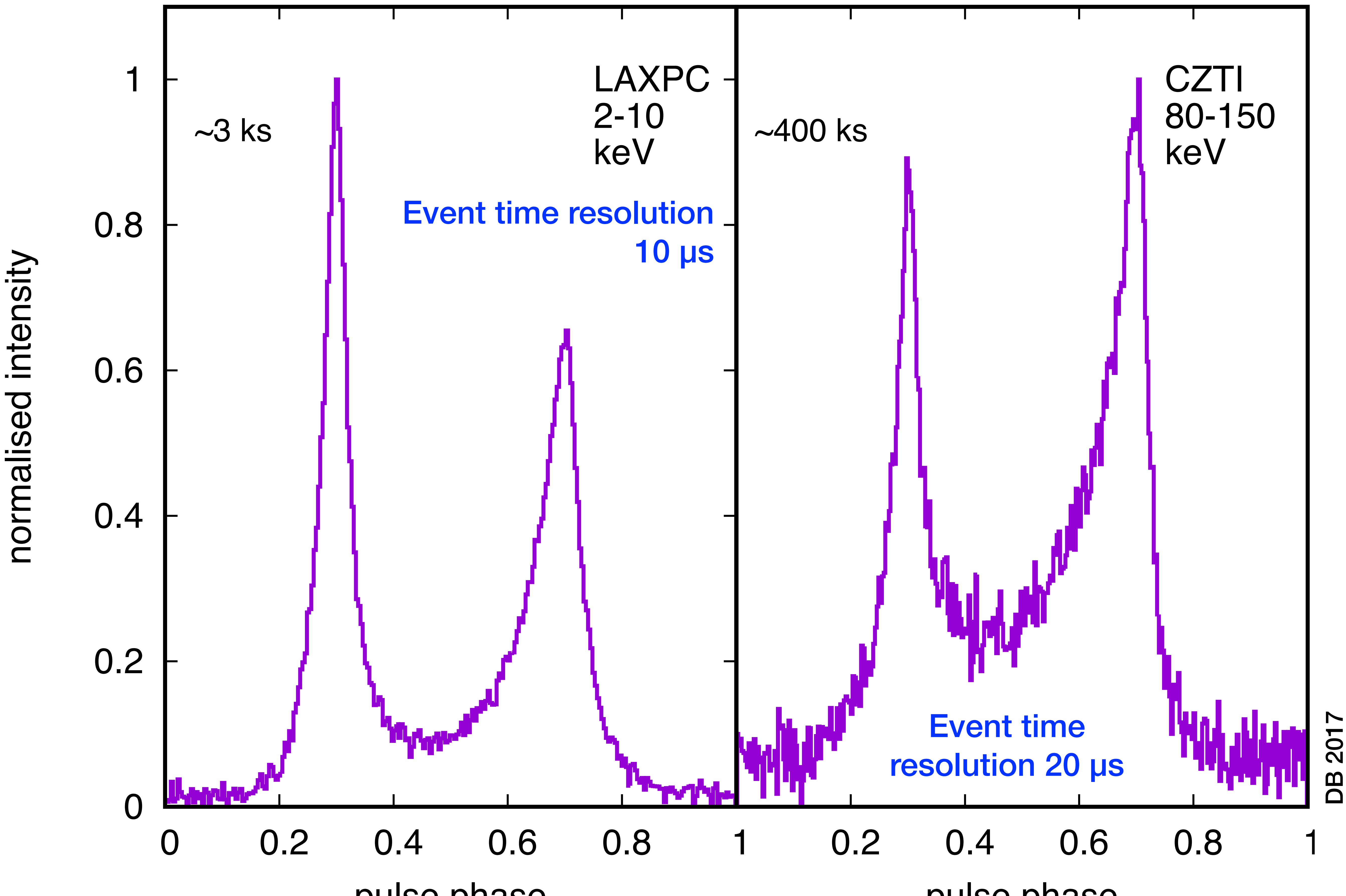

Timing with CZTI

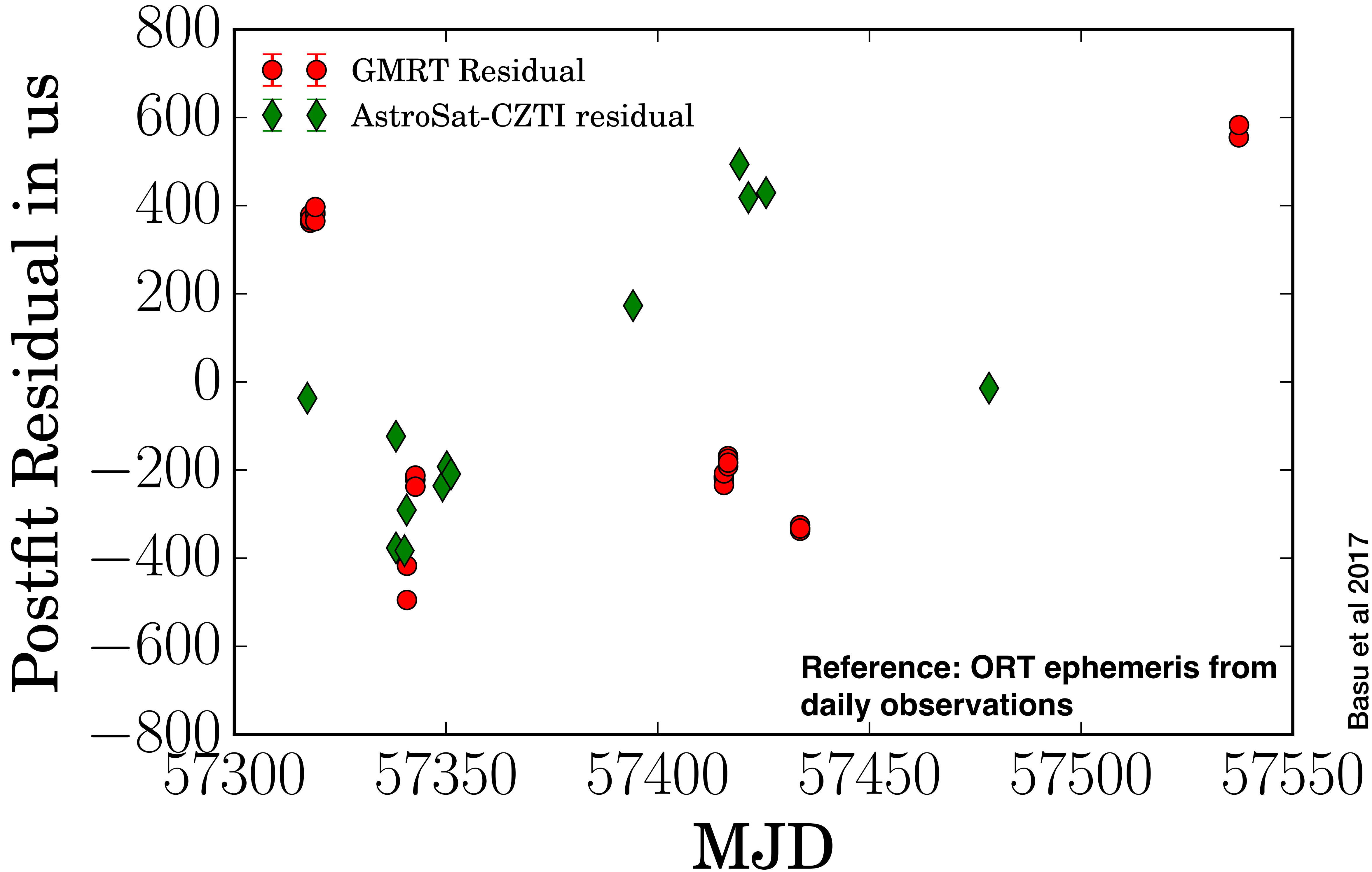

Absolute time calibration using simultaneous radio observations

Stable within ~200 microsec rms

Crab spectral fit with AstroSat instruments

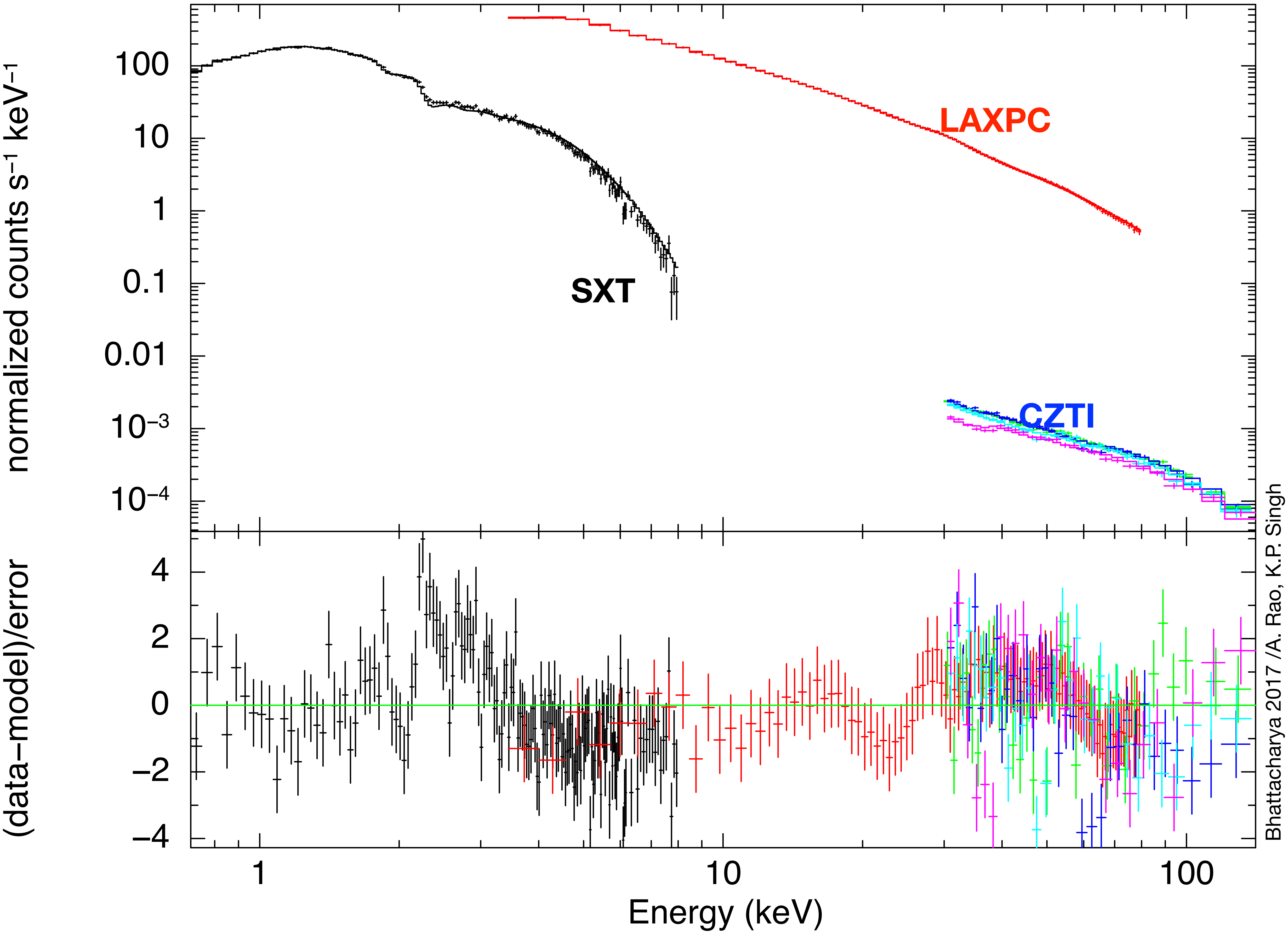

CZTI performs two simultaneous functions

- E < 100 keV: pointed detector, 4.6 deg FOV, targeted observations: *proposed science*
- E > 100 keV: all-sky open detector, high energy transient monitoring: *POC action, shared on web* http://astrosat.iucaa.in/czti/?q=grb

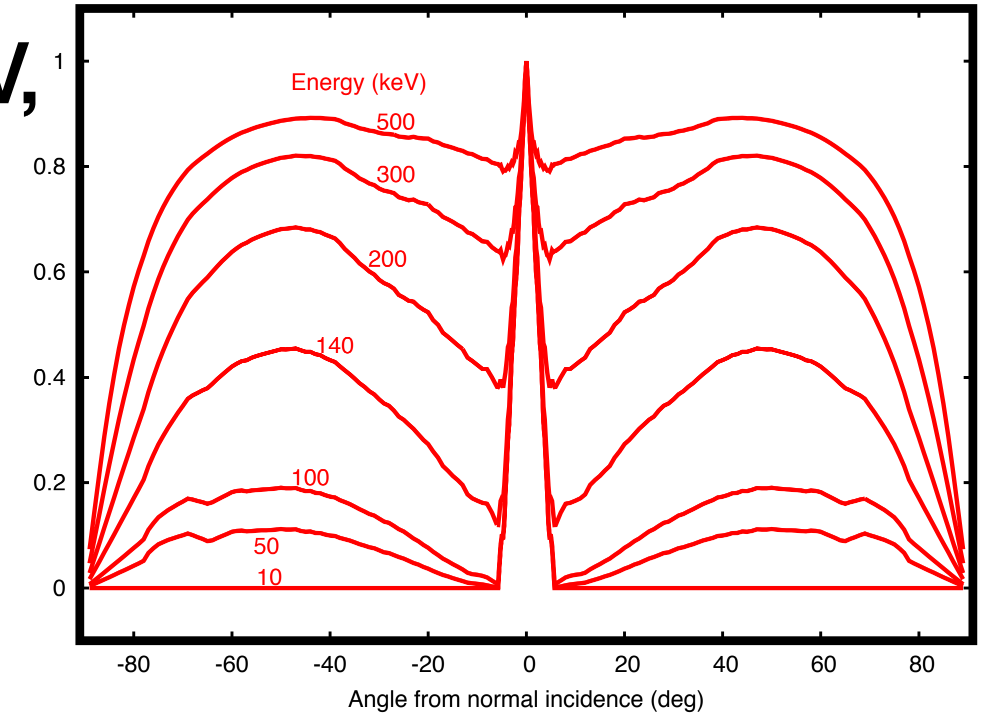

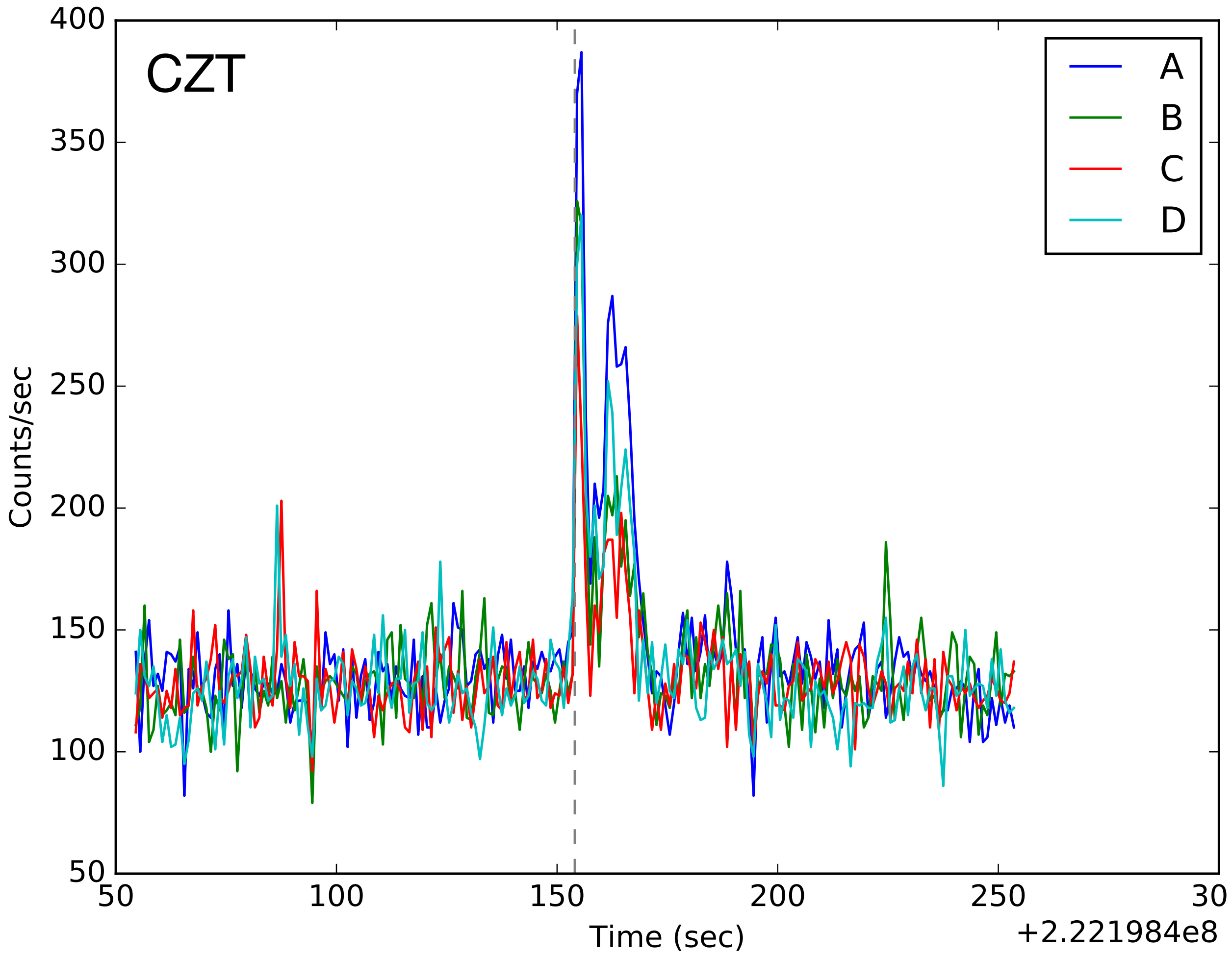

GRB 170115B

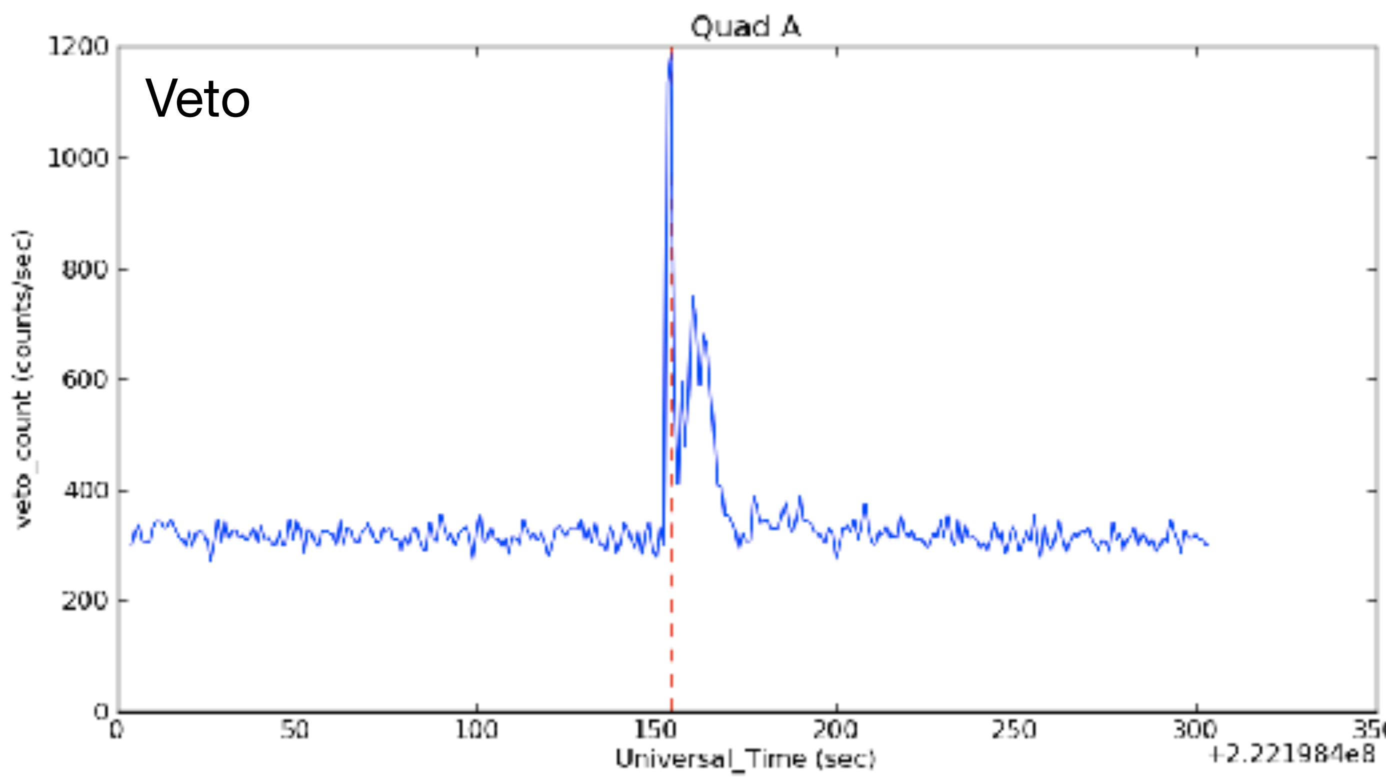

GW counterpart search

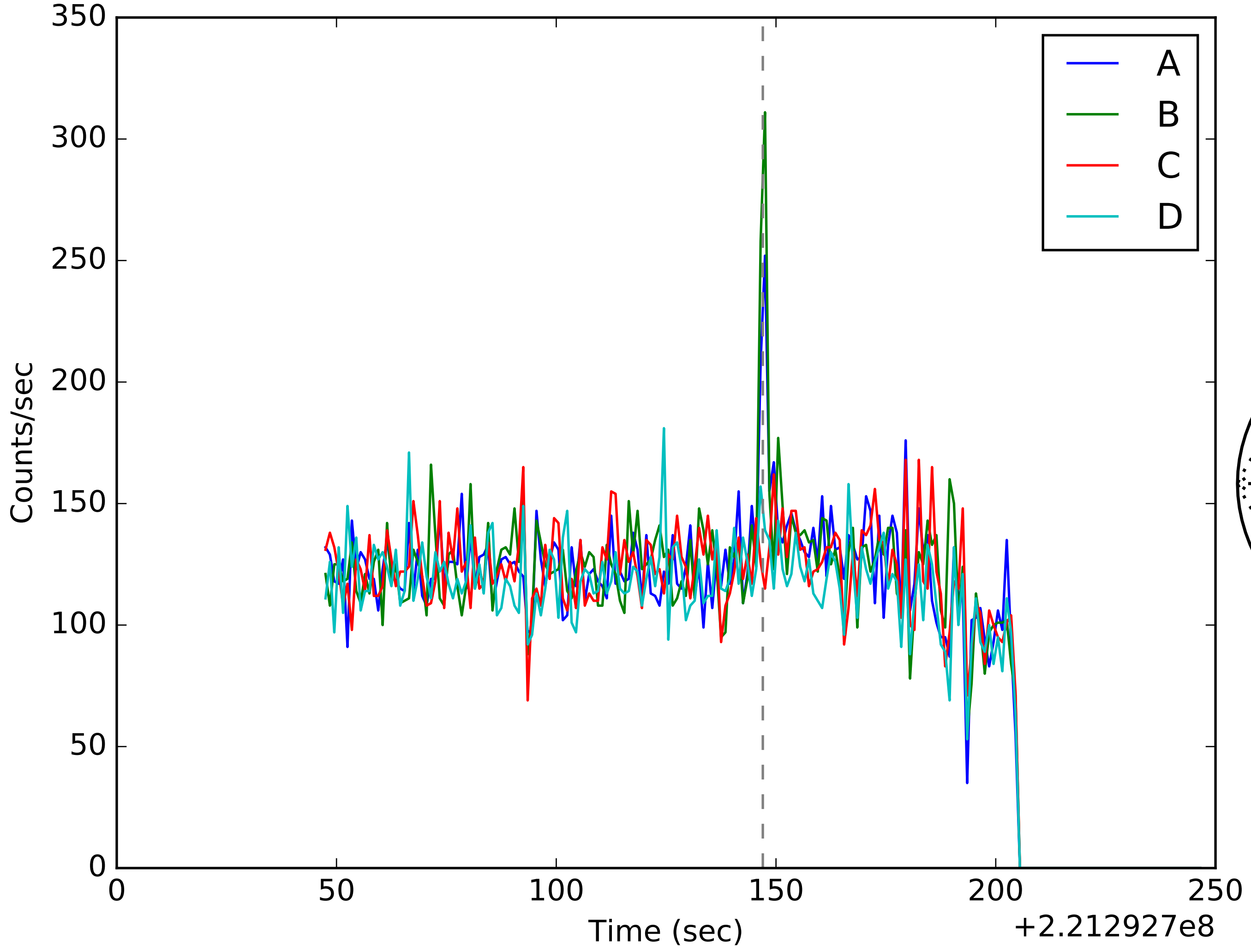

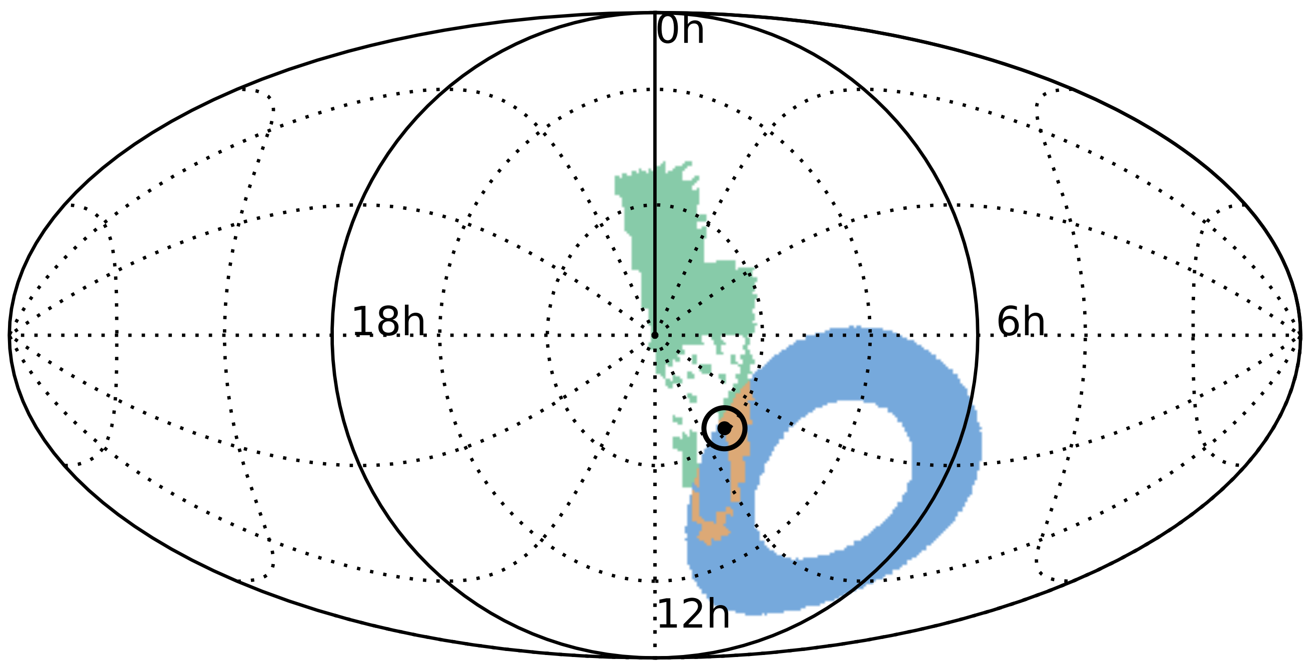

Bhalerao et al 2017

ATLAS 17aeu : purported counterpart of GW 170104; shown by CZTI to be associated with a GRB that occurred 21 h later

GW170817 BNS merger event : No CZTI detection due to Earth occultation

CZTI as Hard X-ray Polarimeter

Phase resolved polarimetry of the Crab in 100-380 keV band using ~800 ks AstroSat CZTI observation

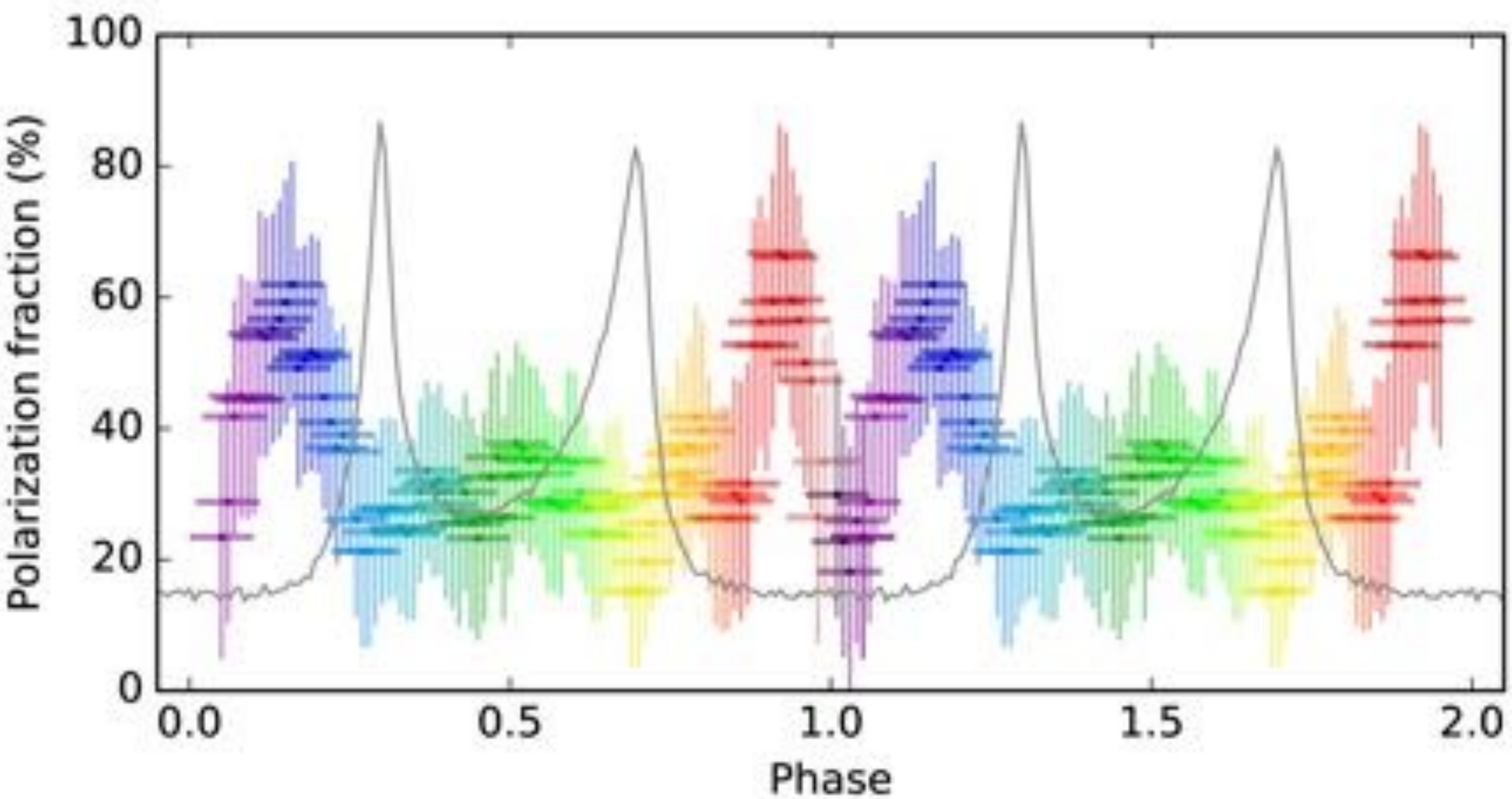

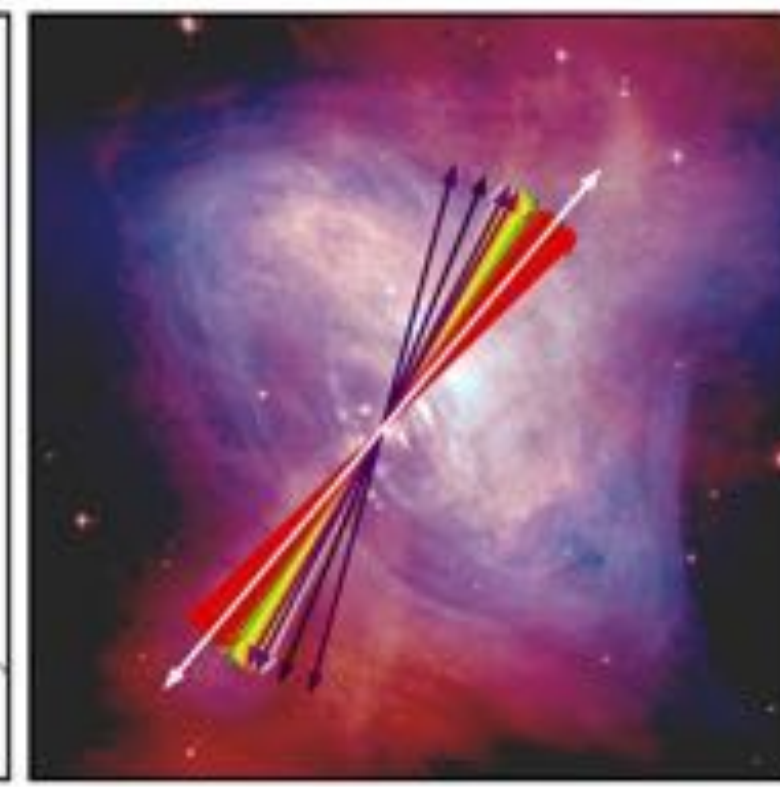

Vadawale et al 2017

CZTI as Hard X-ray Polarimeter

AstroSat/CZTI detects ~60 GRB/y; ~10/y bright enough for polarisation study

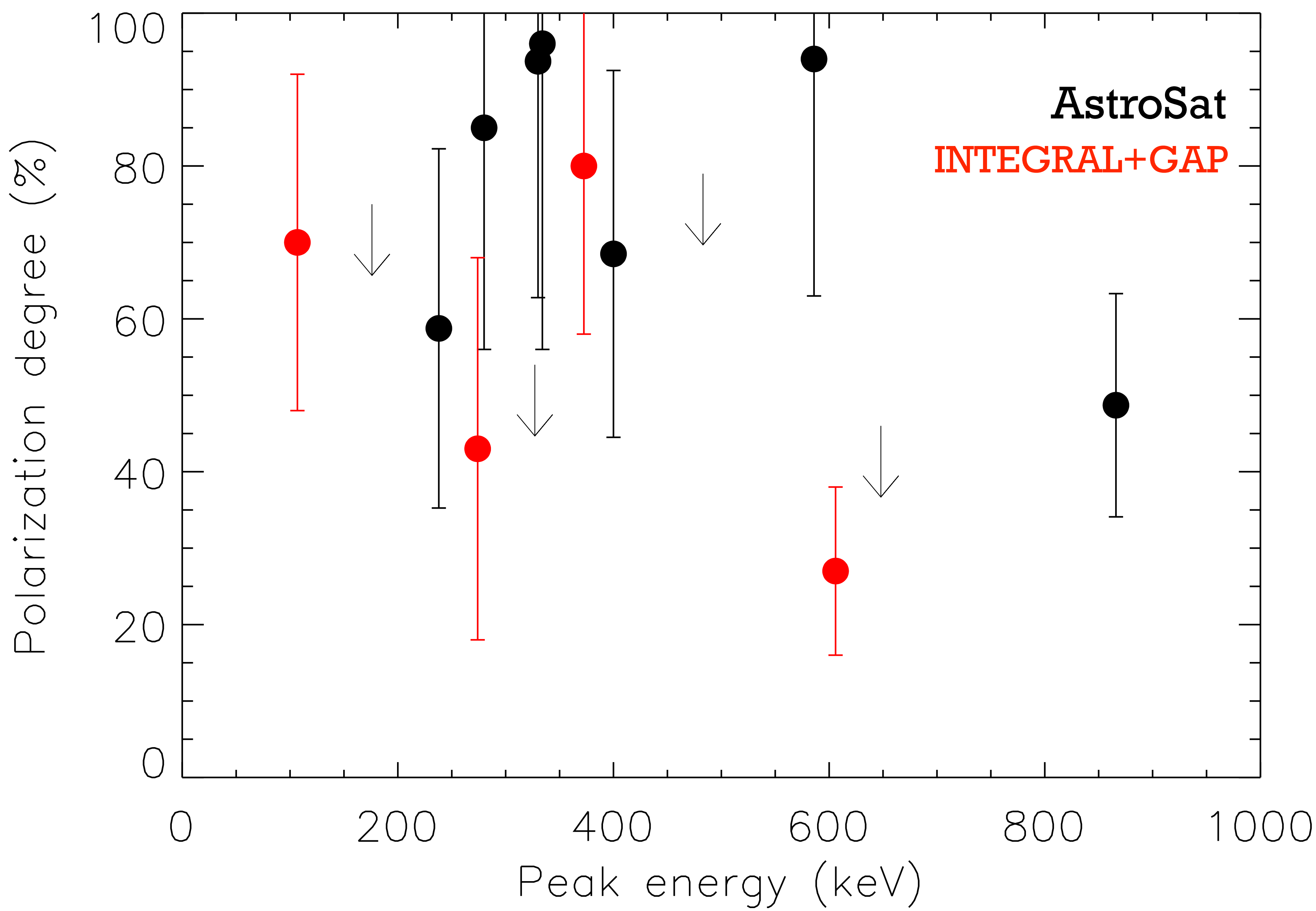

Year 1:

7 detections
4 upper limits

Chattopadhyay et al 2019

GRB 160821A: time resolved spectro-polarimetry